International Journal of Structural Stability and Dynamics
Vol. 13, No. 1 (2013) 1350004 (26 pages)
© World Scientific Publishing Company
DOI: 10.1142/S0219455413500041

World Scientific
www.worldscientific.com

Int. J. Str. Stab. Dyn. 2013.13. Downloaded from www.worldscientific.com
by INDIAN INSTITUTE OF TECHNOLOGY on 08/16/13. For personal use only.

FREE VIBRATION OF FUNCTIONALLY GRADED PLATES WITH A HIGHER-ORDER SHEAR AND NORMAL DEFORMATION THEORY

D. K. JHA

Architectural and Civil Engineering Division
Bhabha Atomic Research Centre, Mumbai 400 085, India
dkjha@barc.gov.in

TARUN KANT

Indian Institute of Technology Bombay, Powai, Mumbai 400 076, India
tkant@civil.iitb.ac.in

R. K. SINGH

Reactor Safety Division
Bhabha Atomic Research Centre, Mumbai 400 085, India
rksingh@barc.gov.in

Received 17 January 2012
Accepted 1 March 2012
Published 6 March 2013

Free vibration analysis of functionally graded elastic, rectangular, and simply supported (diaphragm) plates is presented based on a higher-order shear and normal deformation theory (HOSNT). Although functionally graded materials (FGMs) are highly heterogeneous in nature, they are generally idealized as continua with mechanical properties changing smoothly with respect to the spatial coordinates. The material properties of functionally graded (FG) plates are assumed here to be varying through the thickness of the plate in a continuous manner. The Poisson ratios of the FG plates are assumed to be constant, but their Young's modulii and densities vary continuously in the thickness direction according to the volume fraction of constituents which is mathematically modeled as a power law function. The equations of motion are derived using Hamilton's principle for the FG plates on the basis of a HOSNT assuming varying material properties. Numerical solutions are obtained by the use of Navier solution method. The accuracy of the numerical solutions is first established through comparison with the exact three-dimensional (3D) elasticity solutions and the present solutions are then compared with available solutions of other models.

Keywords: Higher-order shear and normal deformation theory; functionally graded plates; material gradient index; Navier solution; free vibration; natural frequency.

Int. J. Str. Stab. Dyn. 2013.13. Downloaded from www.worldscientific.com
by INDIAN INSTITUTE OF TECHNOLOGY on 08/16/13. For personal use only.

1. Introduction

Functionally graded materials (FGMs) are recently developed advanced composite materials which have potential for wide use in various engineering appliances such as nuclear reactors and high-speed spacecrafts. FGMs are inhomogeneous materials in which the mechanical properties such as Young's modulus of elasticity, Poisson's ratio, shear modulus of elasticity, material density, etc. vary smoothly and continuously in preferred directions. FGMs consisting of metallic and ceramic components are well known to improve the properties of thermal-barrier systems. This is because, cracking or de-lamination, which are often observed in conventional multi-layer systems are avoided due to the smooth transition between the properties of the components. A combination of ceramic and metal is used to make FGMs. The analysis of FGMs has been considered by many researchers in recent years due to the potential of the applications of such materials.

The concept of FGMs was proposed by the Japanese scientists[1] in early nineties. Pagano,[2,3] Srinivas and Rao[4] and Srinivas *et al.*[5] developed the exact solutions of simply supported laminated plates by using three-dimensional (3D) elasticity theory. Their benchmark solutions have proved to be very useful in assessing 2D approximate plate theories by different researchers (see Refs. 6–8). Their methods are valid for laminated plates and shells, where the material properties are piecewise constant, but not applicable for finding solutions of plate problems with continuous inhomogeneity of material properties such as FGMs. Suresh and Mortensen[9] provided an excellent introduction to the fundamentals of FGMs. Intensive studies have been done to analyze the mechanical, thermal and dynamic responses of functionally graded (FG) beams, plates and shells. Tanigawa[10] presented a broad review of the works on FG structures. Praveen and Reddy[11] reported the response of FG ceramic metal plates using a plate finite element formulation. Static behavior of FG rectangular plates based on a third-order shear deformation theory (TSDT) is done by Reddy[12] to show the effects of the material distribution on the deflection and stresses. Javaheri and Eslami[13,14] presented the mechanical and thermal buckling of rectangular FG plates based on the classical and high-order plate theories. Cheng and Batra[15–17] have derived field equations for a FG plate and further these equations are simplified for a simply supported polygonal plate. They established an exact relationship between the deflection of a simply supported FG polygonal plate given by the first-order shear deformation theory (FOST) and TSDT to that of an equivalent homogeneous Kirchhoff plate. They used an asymptotic expansion method for the analysis of 3D thermo-mechanical deformations of FG elliptic plates, rigidly clamped at all the edges with material properties having power-law dependence on the thickness coordinate. In addition, they have also presented the results for the buckling and steady-state vibrations of a simply supported functionally graded polygonal plate based on TSDT. Vel and Batra[18] used the classical plate theory (CPT), FOST and TSDT approximations, for the displacement fields for a simply supported plate assuming trigonometric variation of each displacement components and derived an algebraic equation for the frequencies. The assumed forms of displacements satisfy boundary conditions for only simply supported edge

Int. J. Str. Stab. Dyn. 2013.13. Downloaded from www.worldscientific.com
by INDIAN INSTITUTE OF TECHNOLOGY on 08/16/13. For personal use only.

conditions. Carrera and Brischetto[19] deduced advanced theories for bending analysis of FG plates using the Reissner mixed variational approach. Other recent studies on the 2D models of FG plates may be found in Della Croce *et al.,*[20] GhannadPour *et al.,*[21] Nguyen *et al.,*[22] and Matsunaga.[23] Shahrjerdi *et al.*[24] have studied the free vibration of rectangular simply supported FG plates using second-order shear deformation theory (SSDT). Kumar *et al.*[25] have carried out the free vibration analysis of FG plates using higher-order theory without enforcing zero transverse shear stress conditions on the top and bottom surfaces of the plate using higher-order displacement model. Benachour *et al.*[26] have evaluated the natural frequency of plates made of FG materials by using a four variable refined plate theory with an arbitrary gradient considering only the four number of unknown functions taking account of transverse shear effects and parabolic distribution of the transverse shear strains through the thickness of the plate. Free vibration analysis of FG and composite sandwich plates are carried out by Xiang *et al.*[27] using a displacement model consisting n-order polynomial satisfying zero transverse shear stress boundary conditions at the top and bottom of the plate. Neves *et al.*[28,29] have developed the quasi-3D sinusoidal and hyperbolic shear deformation theories for the bending and free vibration analysis of FG plate accounting through thickness deformations. For inhomogeneous plates, several 3D solutions are also available but most of these works are for laminated plates consisting of homogeneous laminate layers (see Refs. 4, 5 and 30). 3D analytical solutions for FG plates are very useful since they provide benchmark results to assess the accuracy of various 2D plate theories. Main and Spencer[31] constituted a class of exact 3D solutions for FG plates with traction-free surfaces. An asymptotic 3D theory of thermo-mechanical deformations of FG rectangular plates was developed by Reddy and Cheng.[32] Batra and Vel[33] presented a 3D solution for the cylindrical bending vibration of simply supported FG thick plates using displacement fields that identically satisfy boundary conditions to reduce the governing equations to a set of coupled ordinary differential equations. The obtained set of ODEs with variable coefficients is then solved by the power series method. The thermal stresses in a ceramic−metal plate subjected to through-thickness heat flow using the Mori−Tanaka scheme and the classical laminated plate theory were examined by Tsukamoto.[34] Kashtalyan[35] obtained a 3D elasticity solution for a FG simply supported plates using the Plevako[36] general solution methodology for the equilibrium equations of inhomogeneous isotropic media.

In the present article, free vibration analysis of simply supported (diaphragm) FG plates has been carried out using a higher-order shear and normal deformation theory (HOSNT). Hamilton's principle is used to obtain the governing equations of motion for the free vibration of FG plates. The Navier solution method is used as the solution technique for the free vibration problem of FG plate. The material properties are considered to vary in the thickness direction according to power law distribution of constituent volume fraction. The objective of present study is to study the influence of the higher-order terms in the shear deformation theories of FG plate on its natural frequencies. The effect of constituent volume fraction (material grading) of FGMs on free vibration of FG plates is also captured. Natural frequencies evaluated by the present theory are presented in this article. These results are validated first with 3D elasticity solutions and compared with the other models' solutions that are available in the literature.

2. Problem Description and Governing Equations

A linearly-elastic square/rectangular simply supported (diaphragm) FG plate of uniform thickness h is considered as shown in Fig. 1.

A higher-order refined theory for the free vibration analysis of geometrically thick FG plates is presented considering the effects of both the transverse shear and normal strain/stress and the complete material constitutive relation. The theory defines a displacement field in which the in-plane and out-of-plane displacements are nonlinear cubic variations through the plate thickness coordinate. The material properties of the FG plate are assumed to be graded in the thickness direction and the volume fractions of its constituent materials, i.e. ceramic and metal are assumed to follow the power law distribution[11] in the thickness direction, expressed as:

$$V_c = \left(\frac{z}{h} + \frac{1}{2}\right)^k, \quad V_m = 1 - V_c. \tag{1}$$

Here subscripts, m and c indicate the metal and ceramic constituents of FGM, respectively; z represents the thickness coordinate $(-h/2 \leq z \leq h/2)$, and k is the material gradient index $(k \geq 0)$. The variation of the composition of ceramic and metal is linear for $k = 1$. The value of k equal to zero represents a fully ceramic plate. The variation of the ceramic volume fraction function V_c versus nondimensional thickness of plate z/h with different material gradient index k is plotted in Fig. 2.

The mechanical properties of FGM are determined from the volume fraction of the material constituents. The Young's modulus, E and density of material, ρ are

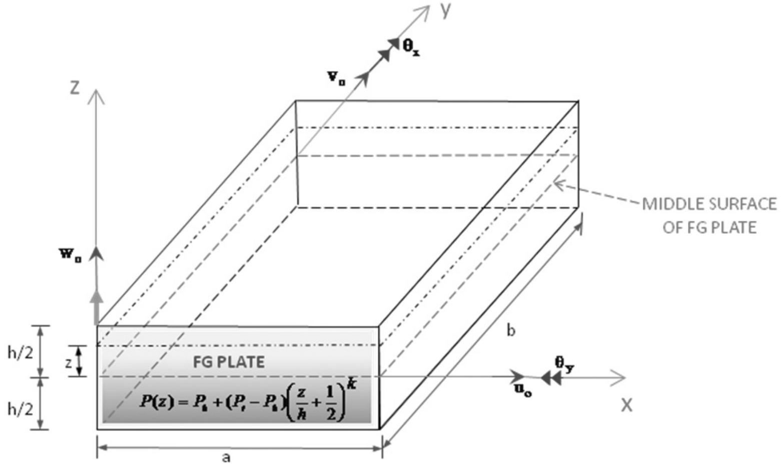

Fig. 1. Geometry of FG plate with positive set of reference axes and its displacement components.

Int. J. Str. Stab. Dyn. 2013.13. Downloaded from www.worldscientific.com
by INDIAN INSTITUTE OF TECHNOLOGY on 08/16/13. For personal use only.

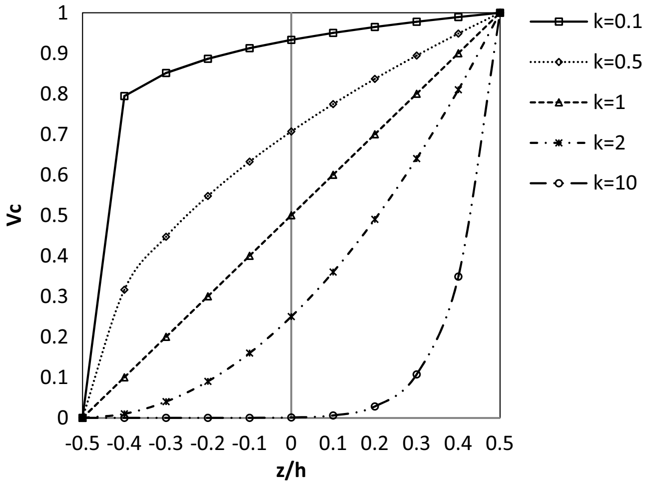

Fig. 2. Variation of ceramic volume fraction with respect to nondimensional thickness of plate with different power index k.

assumed to vary in the thickness direction based on the Voigt's rule over the whole range of the volume fraction.[11] The Poisson' ratio, v is assumed to be constant across the plate thickness. The effective material properties of FGM with two constituents can be expressed as:

$$\begin{aligned} E(z) &= E_c V_c + E_m V_m = E_m + (E_c - E_m)\left(\frac{z}{h} + \frac{1}{2}\right)^k \\ &= E_b + (E_t - E_b)\left(\frac{z}{h} + \frac{1}{2}\right)^k, \end{aligned} \tag{2a}$$

$$\begin{aligned} \rho(z) &= \rho_c V_c + \rho_m V_m = \rho_m + (\rho_c - \rho_m)\left(\frac{z}{h} + \frac{1}{2}\right)^k \\ &= \rho_b + (\rho_t - \rho_b)\left(\frac{z}{h} + \frac{1}{2}\right)^k. \end{aligned} \tag{2b}$$

Here subscripts b and t refer to the bottom $(z = -h/2)$ and top $(z = +h/2)$ surfaces of FG plate. It is clear from the assumed variation expression that the bottom surface of the FG plate is metal rich and the top is ceramic rich in constituents.

2.1. *Displacement-field*

The displacement model assumed here as theoretical basis is based on a higher-order refined theory (see Refs. 37–40) and is re-stated as follows:

$$\begin{aligned} u(x,y,z) &= u_o(x,y) + z\theta_x(x,y) + z^2 u_o^*(x,y) + z^3\theta_x^*(x,y), \\ v(x,y,z) &= v_o(x,y) + z\theta_y(x,y) + z^2 v_o^*(x,y) + z^3\theta_y^*(x,y), \\ w(x,y,z) &= w_o(x,y) + z\theta_z(x,y) + z^2 w_o^*(x,y) + z^3\theta_z^*(x,y). \end{aligned} \tag{3}$$

Int. J. Str. Stab. Dyn. 2013.13. Downloaded from www.worldscientific.com
by INDIAN INSTITUTE OF TECHNOLOGY on 08/16/13. For personal use only.

This model is named as HOSNT12 as it has twelve middle surface parameters giving rise to nonvanishing transverse normal strain term varying quadratically through the thickness. In the above relations, the terms u, v and w are the displacements of a general point $(x,\ y,\ z)$ in the laminate domain in the x, y and z directions, respectively. The parameters u_o, v_o are the in-plane tangential displacements and w_o is the transverse displacement of a point $(x,\ y)$ on the middle surface. The functions θ_x, θ_y are rotations of the normals to the middle surface about y and x axes, respectively. The parameters $u_o^*, v_o^*, w_o^*, \theta_x^*, \theta_y^*, \theta_z^*$ and θ_z are the higher-order terms in the Taylor's series expansion and they represent higher-order transverse cross-sectional deformation modes.

Int. J. Str. Stab. Dyn. 2013.13. Downloaded from www.worldscientific.com
by INDIAN INSTITUTE OF TECHNOLOGY on 08/16/13. For personal use only.

2.2. *Strain–displacement relations*

The general linear strain–displacement relations[41] at any point within a plate are:

$$\varepsilon_x = \frac{\partial u}{\partial x}, \quad \varepsilon_y = \frac{\partial v}{\partial y}, \quad \gamma_{xy} = \frac{\partial u}{\partial y} + \frac{\partial v}{\partial x}, \quad \varepsilon_z = \frac{\partial w}{\partial z},$$
$$\gamma_{yz} = \frac{\partial v}{\partial z} + \frac{\partial w}{\partial y}, \quad \gamma_{xz} = \frac{\partial u}{\partial z} + \frac{\partial w}{\partial x}. \tag{4}$$

The six quantities: three elongations $(\varepsilon_x, \varepsilon_y, \varepsilon_z)$ in three perpendicular directions and three shear strains $(\gamma_{xy}, \gamma_{yz}, \gamma_{xz})$ related to the three orthogonal planes are called components of strain at a point. The strain expressions at a point $\mathrm{P}(x, y, z)$ corresponding to HOSNT12 given by Eq. (3) can be written as below. The strain vector $\boldsymbol{\varepsilon}^z$ is split into two parts, $\boldsymbol{\varepsilon}_{MB}^z$ and $\boldsymbol{\varepsilon}_S^z$. The former corresponds to membrane-bending part while the latter corresponds to transverse shear part. A superscript z signifies that the parameters are defined at a general point P located at a distance z from the reference surface of FG plate.

$$\boldsymbol{\varepsilon}_{MB}^z = \begin{Bmatrix} \varepsilon_x \\ \varepsilon_y \\ \varepsilon_z \\ \gamma_{xy} \end{Bmatrix}^z = \begin{Bmatrix} \varepsilon_{xo} \\ \varepsilon_{yo} \\ \varepsilon_{zo} \\ \varepsilon_{xyo} \end{Bmatrix} + z \begin{Bmatrix} \kappa_x \\ \kappa_y \\ \kappa_z^* \\ \kappa_{xy} \end{Bmatrix} + z^2 \begin{Bmatrix} \varepsilon_{xo}^* \\ \varepsilon_{yo}^* \\ \varepsilon_{zo}^* \\ \varepsilon_{xyo}^* \end{Bmatrix} + z^3 \begin{Bmatrix} \kappa_x^* \\ \kappa_y^* \\ 0 \\ \kappa_{xy}^* \end{Bmatrix}$$
$$= \boldsymbol{\varepsilon}_o + z\boldsymbol{\kappa} + z^2 \boldsymbol{\varepsilon}_o^* + z^3 \boldsymbol{\kappa}^*, \tag{5a}$$

$$\boldsymbol{\varepsilon}_S^z = \begin{Bmatrix} \gamma_{yz} \\ \gamma_{xz} \end{Bmatrix}^z = \begin{Bmatrix} \phi_y \\ \phi_x \end{Bmatrix} + z \begin{Bmatrix} \kappa_{yz} \\ \kappa_{xz} \end{Bmatrix} + z^2 \begin{Bmatrix} \phi_y^* \\ \phi_x^* \end{Bmatrix} + z^3 \begin{Bmatrix} \kappa_{yz}^* \\ \kappa_{xz}^* \end{Bmatrix}$$
$$= \boldsymbol{\varphi}_o + z\boldsymbol{\kappa}_x + z^2 \boldsymbol{\varphi}_o^* + z^3 \boldsymbol{\kappa}_x^*, \tag{5b}$$

Int. J. Str. Stab. Dyn. 2013.13. Downloaded from www.worldscientific.com
by INDIAN INSTITUTE OF TECHNOLOGY on 08/16/13. For personal use only.

where,

$$
\begin{aligned}
(\varepsilon_{xo}, \varepsilon_{yo}, \varepsilon_{xyo}) &= \left(\frac{\partial u_o}{\partial x}, \frac{\partial v_o}{\partial y}, \frac{\partial u_o}{\partial y} + \frac{\partial v_o}{\partial x}\right),\\
(\varepsilon^*_{xo}, \varepsilon^*_{yo}, \varepsilon^*_{xyo}) &= \left(\frac{\partial u^*_o}{\partial x}, \frac{\partial v^*_o}{\partial y}, \frac{\partial u^*_o}{\partial y} + \frac{\partial v^*_o}{\partial x}\right),\\
(\varepsilon_{zo}, \varepsilon^*_{zo}) &= (\theta_z, 3\theta^*_z),\\
(\kappa_{xz}, \kappa_{yz}) &= \left(2u^*_o + \frac{\partial \theta_z}{\partial x}, 2v^*_o + \frac{\partial \theta_z}{\partial y}\right),\\
(\kappa^*_{xz}, \kappa^*_{yz}) &= \left(\frac{\partial \theta^*_z}{\partial x}, \frac{\partial \theta^*_z}{\partial y}\right),\\
(\kappa_x, \kappa_y, \kappa^*_z, \kappa_{xy}) &= \left(\frac{\partial \theta_x}{\partial x}, \frac{\partial \theta_y}{\partial y}, 2w^*_o, \frac{\partial \theta_x}{\partial y} + \frac{\partial \theta_y}{\partial x}\right),\\
(\kappa^*_x, \kappa^*_y, \kappa^*_{xy}) &= \left(\frac{\partial \theta^*_x}{\partial x}, \frac{\partial \theta^*_y}{\partial y}, \frac{\partial \theta^*_x}{\partial y} + \frac{\partial \theta^*_y}{\partial x}\right),\\
(\varphi_x, \varphi^*_x, \varphi_y, \varphi^*_y) &= \left(\theta_x + \frac{\partial w_o}{\partial x}, 3\theta^*_x + \frac{\partial w^*_o}{\partial x}, \theta_y + \frac{\partial w_o}{\partial y}, 3\theta^*_y + \frac{\partial w^*_o}{\partial y}\right).
\end{aligned}
\tag{6}
$$

2.3. *Stress-strain relations*

A FG plate is modeled as an inhomogeneous plate. The material is assumed to be isotropic/orthotropic with varying material properties along plate thickness direction. From linear elasticity theory, the generalized Hooke's law for an orthotropic material can be written as,

$$\boldsymbol{\sigma}'_i = \mathbf{C}_{ij}(z)\boldsymbol{\varepsilon}'_j; \quad i, j = 1 \text{ to } 6. \tag{7}$$

Here $\boldsymbol{\sigma}'_i = (\sigma_1, \sigma_2, \sigma_3, \tau_{12}, \tau_{23}, \tau_{13})^t$ is the stress vector, $\mathbf{C}_{ij}(z)$ is the plate's stiffness matrix and $\boldsymbol{\varepsilon}'_j = (\varepsilon_1, \varepsilon_1, \varepsilon_1, \gamma_{12}, \gamma_{23}, \gamma_{13})^t$ is the engineering strain vector of the material at a distance z from the middle surface with reference to the principal material axes (1, 2, 3). It is assumed here that the structural reference axes (x, y, z) coincide with the principal material axes (1, 2, 3). For an orthotropic FG plate in a 3D state of stress/strain, the constitutive relations given by Eq. (7) can be written in expanded form as follows[8]:

$$
\begin{Bmatrix} \sigma_1 \\ \sigma_2 \\ \sigma_3 \\ \tau_{12} \\ \tau_{23} \\ \tau_{13} \end{Bmatrix}^z = \begin{bmatrix} C_{11} & C_{12} & C_{13} & 0 & 0 & 0 \\ C_{12} & C_{22} & C_{23} & 0 & 0 & 0 \\ C_{13} & C_{23} & C_{33} & 0 & 0 & 0 \\ 0 & 0 & 0 & C_{44} & 0 & 0 \\ 0 & 0 & 0 & 0 & C_{55} & 0 \\ 0 & 0 & 0 & 0 & 0 & C_{66} \end{bmatrix}^z \begin{Bmatrix} \varepsilon_1 \\ \varepsilon_2 \\ \varepsilon_3 \\ \gamma_{12} \\ \gamma_{23} \\ \gamma_{13} \end{Bmatrix}^z \tag{8}
$$

in which,

$$
\begin{aligned}
C_{11} &= \frac{E_1(1-\upsilon_{23}\upsilon_{32})}{\Delta}, \quad C_{12} = \frac{E_1(\upsilon_{21}+\upsilon_{31}\upsilon_{23})}{\Delta} = C_{21},\\
C_{22} &= \frac{E_2(1-\upsilon_{13}\upsilon_{31})}{\Delta}, \quad C_{13} = \frac{E_1(\upsilon_{31}+\upsilon_{21}\upsilon_{32})}{\Delta} = C_{31},\\
C_{33} &= \frac{E_3(1-\upsilon_{12}\upsilon_{21})}{\Delta}, \quad C_{23} = \frac{E_2(\upsilon_{32}+\upsilon_{12}\upsilon_{31})}{\Delta} = C_{32},\\
C_{44} &= G_{12}, \quad C_{55} = G_{23}, \quad C_{66} = G_{13},\\
\Delta &= (1-\upsilon_{12}\upsilon_{21}-\upsilon_{23}\upsilon_{32}-\upsilon_{31}\upsilon_{13}-2\upsilon_{12}\upsilon_{23}\upsilon_{31}).
\end{aligned} \tag{9}
$$

Here, E_1, E_2, E_3 are the Young's modulii and G_{12}, G_{23}, G_{13} are the shear modulii for an orthotropic plate in the three orthogonal planes. υ_{ij} is Poisson's ratio giving the strain in the jth direction caused by a strain in the ith direction.

2.4. *Equations of motion and natural boundary conditions*

The governing equations of motion appropriate for the chosen displacement field, Eq. (3), can be derived using the Hamilton's principle[42] and represented as:

$$
\begin{aligned}
\delta u_o &: \frac{\partial N_x}{\partial x} + \frac{\partial N_{xy}}{\partial y} = \Gamma_1 \ddot{u}_o + \Gamma_2 \ddot{\theta}_x + \Gamma_3 \ddot{u}_o^* + \Gamma_4 \ddot{\theta}_x^*,\\
\delta v_o &: \frac{\partial N_y}{\partial y} + \frac{\partial N_{xy}}{\partial x} = \Gamma_1 \ddot{v}_o + \Gamma_2 \ddot{\theta}_y + \Gamma_3 \ddot{v}_o^* + \Gamma_4 \ddot{\theta}_y^*,\\
\delta w_o &: \frac{\partial Q_x}{\partial x} + \frac{\partial Q_y}{\partial y} = \Gamma_1 \ddot{w}_o + \Gamma_2 \ddot{\theta}_z + \Gamma_3 \ddot{w}_o^* + \Gamma_4 \ddot{\theta}_z^*,\\
\delta \theta_x &: \frac{\partial M_x}{\partial x} + \frac{\partial M_{xy}}{\partial y} - Q_x = \Gamma_2 \ddot{u}_o + \Gamma_3 \ddot{\theta}_x + \Gamma_4 \ddot{u}_o^* + \Gamma_5 \ddot{\theta}_x^*,\\
\delta \theta_y &: \frac{\partial M_y}{\partial y} + \frac{\partial M_{xy}}{\partial x} - Q_y = \Gamma_2 \ddot{v}_o + \Gamma_3 \ddot{\theta}_y + \Gamma_4 \ddot{v}_o^* + \Gamma_5 \ddot{\theta}_y^*,\\
\delta \theta_z &: \frac{\partial S_x}{\partial x} + \frac{\partial S_y}{\partial y} - N_z = \Gamma_2 \ddot{w}_o + \Gamma_3 \ddot{\theta}_z + \Gamma_4 \ddot{w}_o^* + \Gamma_5 \ddot{\theta}_z^*,\\
\delta u_o^* &: \frac{\partial N_x^*}{\partial x} + \frac{\partial N_{xy}^*}{\partial y} - 2S_x = \Gamma_3 \ddot{u}_o + \Gamma_4 \ddot{\theta}_x + \Gamma_5 \ddot{u}_o^* + \Gamma_6 \ddot{\theta}_x^*,\\
\delta v_o^* &: \frac{\partial N_y^*}{\partial y} + \frac{\partial N_{xy}^*}{\partial x} - 2S_y = \Gamma_3 \ddot{v}_o + \Gamma_4 \ddot{\theta}_y + \Gamma_5 \ddot{v}_o^* + \Gamma_6 \ddot{\theta}_y^*,\\
\delta w_o^* &: \frac{\partial Q_x^*}{\partial x} + \frac{\partial Q_y^*}{\partial y} - 2M_z^* = \Gamma_3 \ddot{w}_o + \Gamma_4 \ddot{\theta}_z + \Gamma_5 \ddot{w}_o^* + \Gamma_6 \ddot{\theta}_z^*,\\
\delta \theta_x^* &: \frac{\partial M_x^*}{\partial x} + \frac{\partial M_{xy}^*}{\partial y} - 3Q_x^* = \Gamma_4 \ddot{u}_o + \Gamma_5 \ddot{\theta}_x + \Gamma_6 \ddot{u}_o^* + \Gamma_7 \ddot{\theta}_x^*,\\
\delta \theta_y^* &: \frac{\partial M_y^*}{\partial y} + \frac{\partial M_{xy}^*}{\partial x} - 3Q_y^* = \Gamma_4 \ddot{v}_o + \Gamma_5 \ddot{\theta}_y + \Gamma_6 \ddot{v}_o^* + \Gamma_7 \ddot{\theta}_y^*,\\
\delta \theta_z^* &: \frac{\partial S_x^*}{\partial x} + \frac{\partial S_y^*}{\partial y} - 3N_z^* = \Gamma_4 \ddot{w}_o + \Gamma_5 \ddot{\theta}_z + \Gamma_6 \ddot{w}_o^* + \Gamma_7 \ddot{\theta}_z^*.
\end{aligned} \tag{10}
$$

Int. J. Str. Stab. Dyn. 2013.13. Downloaded from www.worldscientific.com
by INDIAN INSTITUTE OF TECHNOLOGY on 08/16/13. For personal use only.

The inertia terms are defined as

$$\Gamma_1, \Gamma_2, \Gamma_3, \Gamma_4, \Gamma_5, \Gamma_6, \Gamma_7 = \int_{-h/2}^{h/2} \rho(1, z, z^2, z^3, z^4, z^5, z^6)dz. \tag{11}$$

and the boundary conditions are on the edge $x =$ constant,

$$\begin{aligned}
&u_o = \bar{u}_o \quad \text{or} \quad N_x = \bar{N}_x, && v_o = \bar{v}_o \quad \text{or} \quad N_{xy} = \bar{N}_{xy},\\
&w_o = \bar{w}_o \quad \text{or} \quad Q_x = \bar{Q}_x, && \theta_x = \bar{\theta}_x \quad \text{or} \quad M_x = \bar{M}_x,\\
&\theta_y = \bar{\theta}_y \quad \text{or} \quad M_{xy} = \bar{M}_{xy}, && \theta_z = \bar{\theta}_z \quad \text{or} \quad S_x = \bar{S}_x,\\
&u_o^* = \bar{u}_o^* \quad \text{or} \quad N_x^* = \bar{N}_x^*, && v_o^* = \bar{v}_o^* \quad \text{or} \quad N_{xy}^* = \bar{N}_{xy}^*,\\
&w_o^* = \bar{w}_o^* \quad \text{or} \quad Q_x^* = \bar{Q}_x^*, && \theta_x^* = \bar{\theta}_x^* \quad \text{or} \quad M_x^* = \bar{M}_x^*,\\
&\theta_y^* = \bar{\theta}_y^* \quad \text{or} \quad M_{xy}^* = \bar{M}_{xy}^*, && \theta_x^* = \bar{\theta}_x^* \quad \text{or} \quad S_x^* = \bar{S}_x^*
\end{aligned} \tag{12}$$

on the edge $y =$ constant,

$$\begin{aligned}
&u_o = \bar{u}_o \quad \text{or} \quad N_{xy} = \bar{N}_{xy}, && v_o = \bar{v}_o \quad \text{or} \quad N_y = \bar{N}_y,\\
&w_o = \bar{w}_o \quad \text{or} \quad Q_y = \bar{Q}_y, && \theta_x = \bar{\theta}_x \quad \text{or} \quad M_{xy} = \bar{M}_{xy},\\
&\theta_y = \bar{\theta}_y \quad \text{or} \quad M_y = \bar{M}_y, && \theta_z = \bar{\theta}_z \quad \text{or} \quad S_y = \bar{S}_y,\\
&u_o^* = \bar{u}_o^* \quad \text{or} \quad N_{xy}^* = \bar{N}_{xy}^*, && v_o^* = \bar{v}_o^* \quad \text{or} \quad N_y^* = \bar{N}_y^*,\\
&w_o^* = \bar{w}_o^* \quad \text{or} \quad Q_y^* = \bar{Q}_y^*, && \theta_x^* = \bar{\theta}_x^* \quad \text{or} \quad M_{xy}^* = \bar{M}_{xy}^*,\\
&\theta_y^* = \bar{\theta}_y^* \quad \text{or} \quad M_y^* = \bar{M}_y^*, && \theta_z^* = \bar{\theta}_z^* \quad \text{or} \quad S_y^* = \bar{S}_y^*.
\end{aligned} \tag{13}$$

2.5. *Relationship between stress-resultants and middle surface displacements*

The force and moment resultants of FG plate are given by

$$\begin{bmatrix} M_x & M_x^* \\ M_y & M_y^* \\ M_z^* & 0 \\ M_{xy} & M_{xy}^* \end{bmatrix} = \int_{-h/2}^{h/2} \begin{Bmatrix} \sigma_x \\ \sigma_y \\ \sigma_z \\ \tau_{xy} \end{Bmatrix} [\,z \quad z^3\,]dz, \quad \begin{bmatrix} Q_x & Q_x^* \\ Q_y & Q_y^* \end{bmatrix} = \int_{-h/2}^{h/2} \begin{Bmatrix} \tau_{xz} \\ \tau_{yz} \end{Bmatrix} [\,1 \quad z^2\,]dz,$$

$$\begin{bmatrix} N_x & N_x^* \\ N_y & N_y^* \\ N_z & N_z^* \\ N_{xy} & N_{xy}^* \end{bmatrix} = \int_{-h/2}^{h/2} \begin{Bmatrix} \sigma_x \\ \sigma_y \\ \sigma_z \\ \tau_{xy} \end{Bmatrix} [\,1 \quad z^2\,]dz, \quad \begin{bmatrix} S_x & S_x^* \\ S_y & S_y^* \end{bmatrix} = \int_{-h/2}^{h/2} \begin{Bmatrix} \tau_{xz} \\ \tau_{yz} \end{Bmatrix} [\,z \quad z^3\,]dz. \tag{14}$$

Int. J. Str. Stab. Dyn. 2013.13. Downloaded from www.worldscientific.com
by INDIAN INSTITUTE OF TECHNOLOGY on 08/16/13. For personal use only.

Int. J. Str. Stab. Dyn. 2013.13. Downloaded from www.worldscientific.com
by INDIAN INSTITUTE OF TECHNOLOGY on 08/16/13. For personal use only.

In the terms of displacements, we obtain

$$\begin{Bmatrix} N_x \\ N_y \\ N_x^* \\ N_y^* \\ N_z \\ N_z^* \\ M_x \\ M_y \\ M_x^* \\ M_y^* \\ M_z^* \end{Bmatrix} = [\mathbf{A}] \begin{Bmatrix} \frac{\partial u_o}{\partial x} \\ \frac{\partial v_o}{\partial y} \\ \frac{\partial u_o^*}{\partial x} \\ \frac{\partial v_o^*}{\partial y} \\ \theta_z \\ \theta_z^* \\ \frac{\partial \theta_x}{\partial x} \\ \frac{\partial \theta_y}{\partial y} \\ \frac{\partial \theta_x^*}{\partial x} \\ \frac{\partial \theta_y^*}{\partial y} \\ w_o^* \end{Bmatrix} + [\mathbf{A}'] \begin{Bmatrix} \frac{\partial u_o}{\partial y} \\ \frac{\partial v_o}{\partial x} \\ \frac{\partial u_o^*}{\partial y} \\ \frac{\partial v_o^*}{\partial x} \\ \frac{\partial \theta_x}{\partial y} \\ \frac{\partial \theta_y}{\partial x} \\ \frac{\partial \theta_x^*}{\partial y} \\ \frac{\partial \theta_y^*}{\partial x} \end{Bmatrix}, \quad \begin{Bmatrix} N_{xy} \\ N_{xy}^* \\ M_{xy} \\ M_{xy}^* \end{Bmatrix} = [\mathbf{B}'] \begin{Bmatrix} \frac{\partial u_o}{\partial x} \\ \frac{\partial v_o}{\partial y} \\ \frac{\partial u_o^*}{\partial x} \\ \frac{\partial v_o^*}{\partial y} \\ \theta_z \\ \theta_z^* \\ \frac{\partial \theta_x}{\partial x} \\ \frac{\partial \theta_y}{\partial y} \\ \frac{\partial \theta_x^*}{\partial x} \\ \frac{\partial \theta_y^*}{\partial y} \\ w_o^* \end{Bmatrix} + [\mathbf{B}] \begin{Bmatrix} \frac{\partial u_o}{\partial y} \\ \frac{\partial v_o}{\partial x} \\ \frac{\partial u_o^*}{\partial y} \\ \frac{\partial v_o^*}{\partial x} \\ \frac{\partial \theta_x}{\partial y} \\ \frac{\partial \theta_y}{\partial x} \\ \frac{\partial \theta_x^*}{\partial y} \\ \frac{\partial \theta_y^*}{\partial x} \end{Bmatrix},$$

$$\begin{Bmatrix} Q_x \\ Q_x^* \\ S_x \\ S_x^* \end{Bmatrix} = [\mathbf{D}] \begin{Bmatrix} \theta_x \\ \frac{\partial w_o}{\partial x} \\ \theta_x^* \\ \frac{\partial w_o^*}{\partial x} \\ u_o^* \\ \frac{\partial \theta_z}{\partial x} \\ \frac{\partial \theta_z^*}{\partial x} \end{Bmatrix} + [\mathbf{D}'] \begin{Bmatrix} \theta_y \\ \frac{\partial w_o}{\partial y} \\ \theta_y^* \\ \frac{\partial w_o^*}{\partial y} \\ v_o^* \\ \frac{\partial \theta_z}{\partial y} \\ \frac{\partial \theta_z^*}{\partial y} \end{Bmatrix}, \quad \begin{Bmatrix} Q_y \\ Q_y^* \\ S_y \\ S_y^* \end{Bmatrix} = [\mathbf{E}'] \begin{Bmatrix} \theta_x \\ \frac{\partial w_o}{\partial x} \\ \theta_x^* \\ \frac{\partial w_o^*}{\partial x} \\ u_o^* \\ \frac{\partial \theta_z}{\partial x} \\ \frac{\partial \theta_z^*}{\partial x} \end{Bmatrix} + [\mathbf{E}] \begin{Bmatrix} \theta_y \\ \frac{\partial w_o}{\partial y} \\ \theta_y^* \\ \frac{\partial w_o^*}{\partial y} \\ v_o^* \\ \frac{\partial \theta_z}{\partial y} \\ \frac{\partial \theta_z^*}{\partial y} \end{Bmatrix}. \quad (15)$$

The matrices $[\mathbf{A}]$, $[\mathbf{A}']$, $[\mathbf{B}]$, $[\mathbf{B}']$, $[\mathbf{D}]$, $[\mathbf{D}']$, $[\mathbf{E}]$, $[\mathbf{E}']$ are the sub matrices of plate rigidity matrix, and their elements are defined in Appendix A.

3. Analytical Solution

Among all the analytical methods available the Navier solution technique is very simple and easy to use when the plate is of rectangular geometry (side dimensions $= a$ and b, thickness $= h$) with simply supported (diaphragm) edge conditions. This

Int. J. Str. Stab. Dyn. 2013.13. Downloaded from www.worldscientific.com
by INDIAN INSTITUTE OF TECHNOLOGY on 08/16/13. For personal use only.

method of solution for Kirchhoff plate problems of rectangular geometry is well documented.[8]

3.1. *Solution technique*

Navier solution technique using the double Fourier series is described in this section. The boundary conditions for the simply supported (diaphragm) FG plate are:

At edges $x = 0$ and $x = a$:

$$\begin{aligned} &v_o = 0; \quad w_o = 0; \quad \theta_y = 0; \quad \theta_z = 0; \quad M_x = 0; \quad N_x = 0, \\ &v_o^* = 0; \quad w_o^* = 0; \quad \theta_y^* = 0; \quad \theta_z^* = 0; \quad M_x^* = 0; \quad N_x^* = 0. \end{aligned} \tag{16}$$

At edges $y = 0$ and $y = b$:

$$\begin{aligned} &u_o = 0; \quad w_o = 0; \quad \theta_x = 0; \quad \theta_z = 0; \quad M_y = 0; \quad N_y = 0, \\ &u_o^* = 0; \quad w_o^* = 0; \quad \theta_x^* = 0; \quad \theta_z^* = 0; \quad M_y^* = 0; \quad N_y^* = 0. \end{aligned} \tag{17}$$

The generalized displacement field, to satisfy the above boundary conditions, is expanded in double Fourier series as:

$$\begin{aligned}
u_o &= \sum_{m=1}^{\infty}\sum_{n=1}^{\infty} u_{o_{mn}} \cos\alpha_m x \, \sin\beta_n y e^{-i\omega_{mn} t}, \quad & u_o^* &= \sum_{m=1}^{\infty}\sum_{n=1}^{\infty} u_{o_{mn}}^* \cos\alpha_m x \sin\beta_n y e^{-i\omega_{mn} t}, \\
v_o &= \sum_{m=1}^{\infty}\sum_{n=1}^{\infty} v_{o_{mn}} \sin\alpha_m x \cos\beta_n y \, e^{-i\omega_{mn} t}, \quad & v_o^* &= \sum_{m=1}^{\infty}\sum_{n=1}^{\infty} v_{o_{mn}}^* \sin\alpha_m x \cos\beta_n y \, e^{-i\omega_{mn} t}, \\
w_o &= \sum_{m=1}^{\infty}\sum_{n=1}^{\infty} w_{o_{mn}} \sin\alpha_m x \, \sin\beta_n y \, e^{-i\omega_{mn} t}, \quad & w_o^* &= \sum_{m=1}^{\infty}\sum_{n=1}^{\infty} w_{o_{mn}}^* \sin\alpha_m x \, \sin\beta_n y \, e^{-i\omega_{mn} t}, \\
\theta_x &= \sum_{m=1}^{\infty}\sum_{n=1}^{\infty} \theta_{x_{mn}} \cos\alpha_m x \sin\beta_n y \, e^{-i\omega_{mn} t}, \quad & \theta_x^* &= \sum_{m=1}^{\infty}\sum_{n=1}^{\infty} \theta_{x_{mn}}^* \cos\alpha_m x \, \sin\, \beta_n y \, e^{-i\omega_{mn} t}, \\
\theta_y &= \sum_{m=1}^{\infty}\sum_{n=1}^{\infty} \theta_{y_{mn}} \sin\alpha_m x \cos\beta_n y \, e^{-i\omega_{mn} t}, \quad & \theta_y^* &= \sum_{m=1}^{\infty}\sum_{n=1}^{\infty} \theta_{y_{mn}}^* \sin\alpha_m x \cos\beta_n y \, e^{-i\omega_{mn} t}, \\
\theta_z &= \sum_{m=1}^{\infty}\sum_{n=1}^{\infty} \theta_{z_{mn}} \sin\alpha_m x \, \sin\beta_n y \, e^{-i\omega_{mn} t}, \quad & \theta_z^* &= \sum_{m=1}^{\infty}\sum_{n=1}^{\infty} \theta_{z_{mn}}^* \sin\alpha_m x \, \sin\beta_n y \, e^{-i\omega_{mn} t},
\end{aligned} \tag{18}$$

where, $\alpha_m = m\pi/a$, and $\beta_n = n\pi/b$ in which $m, n = 1, 2, 3, \ldots$.

Using the above generalized displacement field and following the standard steps for collecting the coefficients of the twelve displacement degrees of freedom in a

Int. J. Str. Stab. Dyn. 2013.13. Downloaded from www.worldscientific.com
by INDIAN INSTITUTE OF TECHNOLOGY on 08/16/13. For personal use only.

(12×12) system of simultaneous equations we obtain the following eigenvalue problem for any fixed values of m and n:

$$([\mathbf{X}]_{12\times12} - \omega_{mn}^2[\mathbf{M}]_{12\times12})\begin{Bmatrix} u_{o_{mn}} \\ v_{o_{mn}} \\ w_{o_{mn}} \\ \theta_{x_{mn}} \\ \theta_{y_{mn}} \\ \theta_{z_{mn}} \\ u^*_{o_{mn}} \\ v^*_{o_{mn}} \\ w^*_{o_{mn}} \\ \theta^*_{x_{mn}} \\ \theta^*_{y_{mn}} \\ \theta^*_{z_{mn}} \end{Bmatrix}_{12\times1} = \{\mathbf{0}\}. \tag{19}$$

Here, $[\mathbf{X}]$ is the stiffness coefficient matrix whose elements are presented in Appendix B. $[\mathbf{M}]$ is the mass matrix, whose elements are provided in Appendix C. ω_{mn} is the circular natural frequency of vibration of the system associated with mth mode in x-direction and nth mode in y-direction. $u_{o_{mn}}, v_{o_{mn}}, w_{o_{mn}}, \theta_{x_{mn}}, \theta_{y_{mn}}, \theta_{z_{mn}}, u^*_{o_{mn}}, v^*_{o_{mn}}, w^*_{o_{mn}}, \theta^*_{x_{mn}}, \theta^*_{y_{mn}}$, and $\theta^*_{z_{mn}}$ are the unknown coefficients. The above eigenvalue problem can be solved for the various eigenvalues and associated eigenvectors. To obtain nontrivial solution, we must set $|[\mathbf{X}] - \omega_{mn}^2[\mathbf{M}]| = 0$. The real positive roots of Eq. (19) yield the square of the circular natural frequency ω_{mn} corresponding to vibration modes (m, n). The lowest eigenvalue gives the square of the fundamental natural frequency of vibration of FG plate.

4. Numerical Examples

The present higher-order shear and normal deformation theory (HOSNT12) has been used to analyze the free vibration of simply supported (diaphragm) FG plates for different aspect ratios. The material properties are assumed to be graded in the thickness direction as a power law model. A computer program is developed in MATLAB 7.0 based on the theoretical formulation described earlier for the free vibration analysis of FG plates. The parallel modules are also developed for the free vibration analysis of isotropic and orthotropic plates. The natural frequencies for the simply supported (diaphragm) isotropic, orthotropic and FG plates are evaluated using the developed codes. In order to validate the accuracy, the numerical results using present model (HOSNT12) are compared with the other models' solutions, *viz.* CPT, FOST, SSDT, TSDT, refined plate theory (RPT) and the exact 3D elasticity solutions available in the literature. The comparisons of the results are presented in tabular form. The errors in the solutions are computed as follows:

$$\%\ \text{Error} = \left(\frac{\text{Value obtained by a theory}}{\text{Corresponding value by exact solution}} - 1\right) \times 100.$$

Int. J. Str. Stab. Dyn. 2013.13. Downloaded from www.worldscientific.com
by INDIAN INSTITUTE OF TECHNOLOGY on 08/16/13. For personal use only.

The following material properties are used in the analysis:

Isotropic Plates:

$$E = 1\,\text{Gpa}, \quad G = [E/2(1+\upsilon)], \quad \upsilon = 0.3.$$

Non-dimensional frequency, $\hat{\omega}_{mn} = \omega_{mn} h\sqrt{\rho/G}$.

Orthotropic Plates:

$Q_{11} = 160\,\text{GPa}$, $\text{E}_2/E_1 = 0.5250$, $\text{G}_{12}/E_1 = 0.2629$, $\text{G}_{13}/E_1 = 0.1599$, $\text{G}_{23}/E_1 = 0.2688$, $\upsilon_{12} = 0.4405$, $\upsilon_{21} = 0.2312$.

Non-dimensional frequency, $\overline{\omega}_{mn} = \omega_{mn} h\sqrt{\rho/Q_{11}}$.

FG Plates:

Metal (Aluminum): $\text{E}_m = 70\,\text{Gpa}$, $\upsilon = 0.3$, $\rho_m = 2707\,\text{kg/m}^3$

Ceramic (Zirconia): $\text{E}_c = 151\,\text{Gpa}$, $\upsilon = 0.3$, $\rho_c = 3000\,\text{kg/m}^3$

Non-dimensional frequency, $\tilde{\omega}_{mn} = \omega_{mn} h\sqrt{\rho_c/G_c}$.

Natural frequencies (bending frequencies predominantly) using HOSNT12 for isotropic and orthotropic square plates are tabulated in Tables 1 and 2, respectively. The tables also show the 3D elasticity solutions,[4] solutions by Reddy's theory[43,44] named as TSDT, Mindlin's theory which is FOST, CPT taking into account rotary inertias, results using the displacement model considered by Senthilnathan *et al.*[45] and results of RPT.[46] Present results are obtained using same values of m and n as those used for obtaining results using 3D elasticity exact theory.[4]

The HOSNT12 has been used to evaluate the fundamental natural frequency of simply supported (diaphragm) FG plates for different values of aspect ratios (b/a). The exact values of nondimensional natural frequencies of simply supported (diaphragm) isotropic plates using 3D elasticity theory are available for $b/a = 1$ and $a/h = 10$ in Ref. 4. The exact value of the same is available for $b/a = \sqrt{2}$ and $a/h = 10$ in Ref. 47. The nondimensional natural frequencies of simply supported (diaphragm) isotropic plates are available using CPT without and with rotary inertia (CPT1 and CPT2), FOST, TSDT in various references. A comparison between these results and the presented results (HOSNT12) is shown in Table 3. The comparison shows that the presented results are much closed to the 3D elasticity solutions. The influence of constituents volume fraction on the natural frequencies of FG plate is studied by varying the value of material gradient index, k. As can be seen from the presented results, the natural frequencies decreased with increasing the value of power index, k. The natural frequencies of rectangular plate with $b = \sqrt{2}a$ are smaller than the other one, $b = a$.

The nondimensional fundamental natural frequency of square and rectangular FG plates is presented in Table 4 for different side-to-thickness (a/h) ratios using HOSNT12. In order to obtain the frequencies of simply supported (diaphragm) FG plates with various aspect ratio (b/a), thickness ratio (a/h) and material gradient index (k), a separate formulation for FOST and associated computer program has also been developed. The results of FOST considering the shear correction factor are also provided in Table 4. This has especially been done in order to compare the HOSNT12 results with FOST results for FG plates. The results show that for a/h more than 10, i.e. thin plates, FOST and HOSNT12 results are very closed. But, for

Int. J. Str. Stab. Dyn. 2013.13. Downloaded from www.worldscientific.com
by INDIAN INSTITUTE OF TECHNOLOGY on 08/16/13. For personal use only.

Table 1. Comparison of nondimensional natural frequencies $\hat{\omega}_{mn}$ of simply supported (diaphragm) isotropic square plate ($a/h = 10, b/a = 1.0$).

		Nondimensional natural frequencies $\hat{\omega}_{mn}$ by various theories							
m	n	Exact[a] (3D elasticity)	Present (HOSNT12)	Reddy[b] (TSDT)	Reissner[b] (FOST)	Reissner[b] (FOST) using shear correction factor (5/6)	CPT[b]	Senthilnathan *et al.*[c]	RPT[d]
1	1	0.0932	0.0932 (0.00)	0.0930 (−0.21)	0.0934 (0.21)	0.0930 (−0.21)	0.0955 (2.47)	0.0930 (−0.21)	0.0930 (−0.21)
1	2	0.2226	0.2226 (0.00)	0.2220 (−0.27)	0.2241 (0.67)	0.2219 (−0.28)	0.2360 (6.02)	0.2220 (−0.27)	0.2220 (−0.27)
2	2	0.3421	0.3421 (0.00)	0.3406 (−0.44)	0.3454 (0.96)	0.3406 (−0.44)	0.3732 (9.09)	0.3406 (−0.44)	0.3406 (−0.44)
1	3	0.4171	0.4172 (0.02)	0.4151 (−0.48)	0.4220 (1.17)	0.4149 (−0.53)	0.4629 (10.98)	0.4150 (−0.50)	0.4151 (−0.48)
2	3	0.5239	0.5240 (0.02)	0.5208 (−0.59)	0.5312 (1.39)	0.5206 (−0.63)	0.5951 (13.59)	0.5208 (−0.59)	0.5208 (−0.59)
1	4	—	0.6573	0.6525	0.6680	0.6520	0.7668	0.6524	0.6525
3	3	0.6889	0.6892 (0.04)	0.6839 (−0.73)	0.7008 (1.73)	0.6834 (−0.80)	0.8090 (17.43)	0.6839 (−0.73)	0.6840 (−0.71)
2	4	0.7511	0.7515 (0.05)	0.7454 (−0.76)	0.7649 (1.84)	0.7447 (−0.85)	0.8926 (18.84)	0.7453 (−0.77)	0.7454 (−0.76)
3	4	—	0.8992	0.8908	0.9172	0.8896	1.0965	0.8908	0.8908
1	5	0.9268	0.9275 (0.08)	0.9187 (−0.87)	0.9465 (2.13)	0.9174 (−1.01)	1.1365 (22.63)	0.9186 (−0.88)	0.9187 (−0.87)
2	5	—	1.0102	1.0000	1.0321	0.9984	1.2549	1.0000	1.0001
4	4	1.0889	1.0899 (0.09)	1.0784 (−0.96)	1.1146 (2.36)	1.0764 (−0.96)	1.3716 (25.96)	1.0784 (−0.96)	1.0785 (−0.96)
3	5	—	1.1416	1.291	1.1681	1.1269	1.4475	1.1292	1.1292

Numbers inside the bracket is the % error computed.
—Against an entry indicates that the results/data are not available.
[a]Taken from Ref. 4.
[b]Results using these theories are computed independently and are found same as reported in various references.
[c]Taken from Ref. 45.
[d]Taken from Ref. 46.

Int. J. Str. Stab. Dyn. 2013.13. Downloaded from www.worldscientific.com
by INDIAN INSTITUTE OF TECHNOLOGY on 08/16/13. For personal use only.

Table 2. Comparison of nondimensional natural frequencies $\overline{\omega}_{mn}$ of simply supported (diaphragm) orthotropic square plate ($a/h = 10$, $b/a = 1.0$).

		Nondimensional natural frequencies $\overline{\omega}_{mn}$ by various theories						
m	n	Exact[a] (3D elasticity)	Present (HOSNT12)	Reddy[b] (TSDT)	Reissner[b] (FOST) using shear correction factor (5/6)	CPT[b]	Senthilnathan *et al.*[c]	RPT[d]
1	1	0.0474	0.0475 (0.22)	0.0476 (0.42)	0.0476 (0.42)	0.0497 (4.85)	0.0478 (0.84)	0.0477 (0.63)
1	2	0.1033	0.1038 (0.53)	0.1041 (0.77)	0.1041 (0.77)	0.1120 (8.42)	0.1049 (1.55)	0.1040 (0.68)
2	2	0.1188	0.1188 (0.02)	0.1189 (0.08)	0.1188 (0.00)	0.1354 (13.97)	0.1198 (0.84)	0.1198 (0.84)
1	3	0.1694	0.1696 (0.13)	0.1698 (0.24)	0.1698 (0.24)	0.1987 (17.30)	0.1726 (1.89)	0.1722 (1.65)
2	3	0.1888	0.1900 (0.63)	0.1906 (0.95)	0.1905 (0.90)	0.2154 (14.09)	0.1919 (1.64)	0.1898 (0.53)
1	4	0.2180	0.2180 (0.01)	0.2181 (0.05)	0.2178 (−0.09)	0.2779 (27.48)	0.2197 (0.78)	0.2197 (0.78)
3	3	0.2475	0.2480 (0.22)	0.2487 (0.48)	0.2485 (0.40)	0.3029 (22.38)	0.2533 (2.34)	0.2520 (1.82)
2	4	0.2624	0.2625 (0.03)	0.2626 (0.08)	0.2623 (−0.04)	0.3418 (30.26)	0.2677 (2.02)	0.2675 (1.94)
3	4	0.2969	0.2985 (0.54)	0.2995 (0.88)	0.2994 (0.84)	0.3599 (21.22)	0.3012 (1.45)	0.2980 (0.37)
1	5	0.3319	0.3319 (0.01)	0.3320 (0.03)	0.3340 (0.63)	0.4773 (43.81)	0.3340 (0.63)	0.3340 (0.63)
2	5	0.3320	0.3323 (0.09)	0.3326 (0.18)	0.3321 (0.03)	0.4470 (34.64)	0.3414 (2.83)	0.3407 (2.62)
4	4	0.3476	0.3485 (0.25)	0.3495 (0.55)	0.3491 (0.43)	0.4480 (28.88)	0.3558 (2.36)	0.3534 (1.67)
3	5	0.3707	0.3707 (0.01)	0.3708 (0.03)	0.3698 (−0.24)	0.5415 (46.07)	0.3775 (1.83)	0.3774 (1.81)

Numbers inside the bracket is the % error computed.
[a]Taken from Ref. 4.
[b]Results using these theories are computed independently and are found same as reported in various references.
[c]Taken from Ref. 45.
[d]Taken from Ref. 46.

Int. J. Str. Stab. Dyn. 2013.13. Downloaded from www.worldscientific.com
by INDIAN INSTITUTE OF TECHNOLOGY on 08/16/13. For personal use only.

Table 3. Comparison of nondimensional natural frequencies $\tilde{\omega}_{mn}(m = n = 1)$ of simply supported (diaphragm) FG plate for different material distribution ($a/h = 10$, $b/a = 1.0$ and $\sqrt{2}$).

Aspect ratio and thickness ratio	Theory	Material gradient index (k)						
		0 (Ceramic)	0.1	0.5	1	2	10	100 (Metal)
$b/a = 1$	Exact[a]	0.0932	—	—	—	—	—	—
$a/h = 10$	CPT1[b]	0.0955 (2.47)	—	—	—	—	—	—
	CPT2[b]	0.0963 (3.33)	—	—	—	—	—	—
	FOST[b]	0.0934 (0.21)	0.0908	0.0841	0.0802	0.0774	0.0731	0.0680
	FOST[b] using shear correction factor (5/6)	0.0930 (−0.21)	0.0904	0.0837	0.0798	0.0770	0.0727	0.0677
	HOSNT12	0.0932 (0.00)	0.0906	0.0839	0.0799	0.0770	0.0727	0.0678
$b/a = \sqrt{2}$	Exact[e]	0.0704	—	—	—	—	—	—
$a/h = 10$								
	CPT1[b]	0.0718 (1.99)	—	—	—	—	—	—
	CPT2[b]	0.0722 (2.56)	—	—	—	—	—	—
	FOST[b]	0.0706 (0.28)	0.0686	0.0635	0.0606	0.0585	0.0552	0.0514
	FOST[b] using shear correction factor (5/6)	0.0704 (0.00)	0.0684	0.0633	0.0604	0.0582	0.0550	0.0512
	HOSNT12	0.0704 (0.00)	0.0685	0.0634	0.0604	0.0583	0.0550	0.0512

Numbers inside the bracket is the % error computed.
Against an entry indicates that the results/data are not available.
[a]Taken from Ref. 4.
[b]Results using these theories are computed independently and are found same as reported in various references.
[e]Taken from Ref. 47.

Int. J. Str. Stab. Dyn. 2013.13. Downloaded from www.worldscientific.com
by INDIAN INSTITUTE OF TECHNOLOGY on 08/16/13. For personal use only.

Table 4. Nondimensional natural frequencies $\tilde{\omega}_{mn}(m = n = 1)$ of simply supported (diaphragm) FG plate for different aspect ratios (b/a) and thickness ratios (a/h) for different material distribution.

			Material gradient index (k)						
Aspect ratio (b/a)	Theory	Thickness ratio (a/h)	0 (Ceramic)	0.1	0.5	1	2	10	100 (Metal)
1	FOST (using shear correction factor 5/6)	2	1.5597	1.5212	1.4163	1.3480	1.2883	1.1959	1.1300
		5	0.3454	0.3361	0.3116	0.2969	0.2857	0.2686	0.2511
		10	0.0934	0.0908	0.0841	0.0802	0.0774	0.0731	0.0680
		20	0.0239	0.0232	0.0215	0.0205	0.0198	0.0187	0.0174
		50	0.0038	0.0037	0.0035	0.0033	0.0032	0.0030	0.0028
		100	0.0010	0.0009	0.0009	0.0008	0.0008	0.0008	0.0007
	HOSNT12	2	1.5185	1.4836	1.3851	1.3162	1.2482	1.1481	1.0990
		5	0.3421	0.3331	0.3091	0.2942	0.2823	0.2646	0.2485
		10	0.0932	0.0906	0.0839	0.0799	0.0770	0.0727	0.0678
		20	0.0239	0.0232	0.0215	0.0205	0.0198	0.0187	0.0174
		50	0.0038	0.0037	0.0035	0.0033	0.0032	0.0030	0.0028
		100	0.0010	0.0009	0.0009	0.0008	0.0008	0.0008	0.0007
$\sqrt{2}$	FOST (using shear correction factor 5/6)	2	1.2590	1.2274	1.1418	1.0869	1.0401	0.9678	0.9127
		5	0.2655	0.2583	0.2393	0.2280	0.2196	0.2068	0.1930
		10	0.0706	0.0686	0.0635	0.0606	0.0585	0.0552	0.0514
		20	0.0180	0.0174	0.0161	0.0154	0.0149	0.0141	0.0131
		50	0.0029	0.0028	0.0026	0.0025	0.0024	0.0023	0.0021
		100	0.0007	0.0007	0.0006	0.0006	0.0006	0.0006	0.0005
	HOSNT12	2	1.2292	1.2002	1.1192	1.0638	1.0108	0.9330	0.8902
		5	0.2634	0.2564	0.2378	0.2264	0.2175	0.2043	0.1915
		10	0.0704	0.0685	0.0634	0.0604	0.0583	0.0550	0.0512
		20	0.0179	0.0174	0.0161	0.0154	0.0149	0.0140	0.0131
		50	0.0029	0.0028	0.0026	0.0025	0.0024	0.0023	0.0021
		100	0.0007	0.0007	0.0006	0.0006	0.0006	0.0006	0.0005

Int. J. Str. Stab. Dyn. 2013.13. Downloaded from www.worldscientific.com
by INDIAN INSTITUTE OF TECHNOLOGY on 08/16/13. For personal use only.

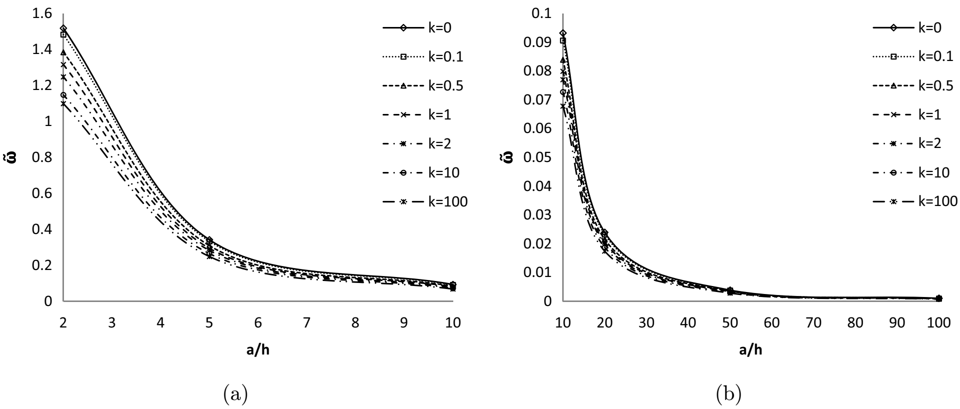

Fig. 3. Nondimensional fundamental natural frequency $\tilde{\omega}_{mn}(m = n = 1)$ of simply supported (diaphragm) FG square plates ($b = a$) as a function of side-to thickness ratio (a/h) for different "k" using HOSNT12. (a) for $a/h = 2$ to 10; (b) for $a/h = 10$ to 100.

thick plates, i.e. a/h less than 10, the natural frequencies by HOSNT12 and FOST are different. The effectiveness of HOSNT12 can be easily observed by the presented results for thick FG plates.

The nondimensional fundamental natural frequency of simply supported (diaphragm) FG plates against material gradient index, k for various side-to-thickness ratio, a/h and for $b/a = 1$ and $\sqrt{2}$ are plotted in Figs. 3 and 4 based on HOSNT12. The fundamental natural frequency decreases significantly with increase of the metal percentage of FGM. It is basically due to the fact that the Young's modulus of ceramic is higher than metal. It is worth noting that, as a/h increases, the natural frequencies decreases because of the decrease in stiffness of the plate. Also, when the ratio a/h is small (thicker plates), the difference between the results of HOSNT12 and FOST results are more.

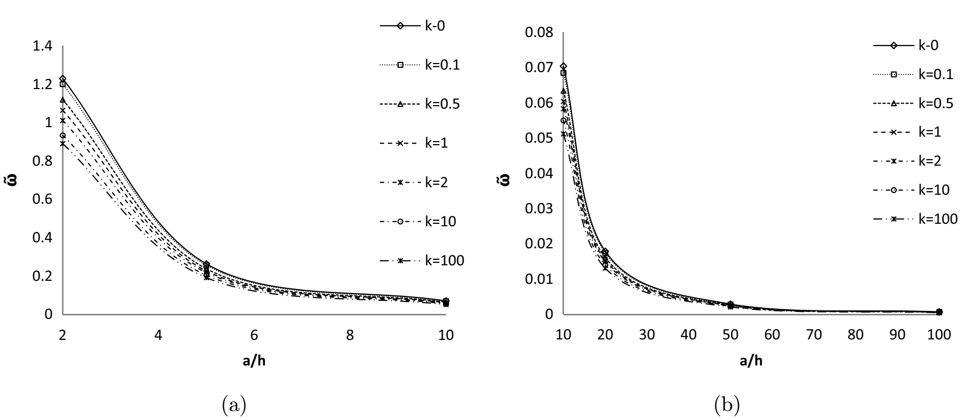

Fig. 4. Nondimensional fundamental natural frequency $\tilde{\omega}_{mn}(m = n = 1)$ of simply supported (diaphragm) FG rectangular plates ($b = \sqrt{2}a$) as a function of side-to-thickness ratio (a/h) for different "k" using HOSNT12. (a) for $a/h = 2$ to 10; (b) for $a/h = 10$ to 100.

Int. J. Str. Stab. Dyn. 2013.13. Downloaded from www.worldscientific.com
by INDIAN INSTITUTE OF TECHNOLOGY on 08/16/13. For personal use only.

Table 5. Nondimensional fundamental natural frequencies $\tilde{\omega}_{mn}$ and $\tilde{\tilde{\omega}}_{mn}$ of simply supported (diaphragm) FG plates using HOSNT12.

Aspect ratio (b/a)	Thickness ratio (a/h)	Material gradient index (k)							
		$k=0$ (Ceramic)		$k=1$		$k=10$		$k=100$ (Metal)	
		$\tilde{\omega}_{mn}$	$\tilde{\tilde{\omega}}_{mn}$	$\tilde{\omega}_{mn}$	$\tilde{\tilde{\omega}}_{mn}$	$\tilde{\omega}_{mn}$	$\tilde{\tilde{\omega}}_{mn}$	$\tilde{\omega}_{mn}$	$\tilde{\tilde{\omega}}_{mn}$
$b/a=1$	2	1.5185	3.7670	1.3160	3.2650	1.1481	2.8482	1.0990	2.7264
	5	0.3421	5.3042	0.2943	4.5621	0.2646	4.1022	0.2485	3.8535
	10	0.0932	5.7713	0.0799	4.9573	0.0727	4.5067	0.0678	4.2029
	20	0.0239	5.9219	0.0205	5.0780	0.0187	4.6332	0.0174	4.3104
	50	0.0038	5.9650	0.0033	5.1138	0.0030	4.6710	0.0028	4.3424
	100	0.0010	5.9713	0.0008	5.1190	0.0008	4.6765	0.0007	4.3470
$b/a=\sqrt{2}$	2	1.2292	3.0493	1.0638	2.6389	0.9330	2.3144	0.8902	2.2083
	5	0.2634	4.0845	0.2264	3.5107	0.2043	3.1668	0.1915	2.9686
	10	0.0704	4.3679	0.0604	3.7472	0.0550	3.4106	0.0512	3.1782
	20	0.0179	4.4510	0.0154	3.8164	0.0140	3.4832	0.0131	3.2398
	50	0.0029	4.4753	0.0025	3.8367	0.0023	3.5046	0.0021	3.2579
	100	0.0007	4.4788	0.0006	3.8396	0.0006	3.5077	0.0005	3.2605

There is one another kind of nondimensionalization of natural frequency available in the literature (Refs. 24–27). The nondimensional frequency in these references is defined as $\tilde{\tilde{\omega}}_{mn} = (\omega_{mn}a^2/h)\sqrt{\rho_c/E_c}$. This kind of nondimensional fundamental natural frequency, $\tilde{\tilde{\omega}}_{mn}(m=n=1)$ is evaluated using HOSNT12 for various k, a/h and b/a, and is presented in Table 5.

It can be clearly seen from the presented results that this nondimensional frequency also decreases with the increase of material gradient index (k). Here, it is interesting to note that this nondimensional frequency increases with the increase of thickness ratio (a/h) of the plate. This is because of the fact that thickness ratio (a/h) term is getting multiplied into the nondimensional frequency parameter.

In Table 6, nondimensional frequency parameter $\tilde{\tilde{\omega}}_{mn}$ of rectangular FG plates based on HOSNT12 is compared with the SSDT solutions by Shahrjerdi *et al.*[24]

Table 6. Natural frequencies of rectangular FG plate ($b/a=2$, $a/h=10$).

$m\times n$	Mode	Nondimensional natural frequencies, $\tilde{\tilde{\omega}}_{mn} = (\omega_{mn}a^2/h)\sqrt{\rho_c/E_c}$							
		$k=0$		$k=0.5$		$k=1$		$k=2$	
		SSDT[f]	HOSNT12	SSDT[f]	HOSNT12	SSDT[f]	HOSNT12	SSDT[f]	HOSNT12
1×1	1	3.6983	3.6911	3.3713	3.3664	3.2225	3.2179	3.1354	3.1291
1×2	2	5.8498	5.8323	5.3359	5.3238	5.1002	5.0886	4.9594	4.9434
2×1	3	12.0345	11.965	10.9940	10.946	10.5062	10.461	10.1985	10.137
2×2	4	14.0144	13.921	12.8103	12.745	12.2421	12.180	11.8784	11.794
2×3	5	17.2325	17.096	15.7660	15.668	15.0670	14.973	14.6092	14.481
3×2	6	26.3462	26.051	24.1494	23.941	23.0749	22.876	22.3273	22.059
3×3	7	29.2257	28.871	26.8100	26.554	25.6184	25.372	24.7781	24.446

[f]Taken from Shahrjerdi *et al.*[24]

Int. J. Str. Stab. Dyn. 2013.13. Downloaded from www.worldscientific.com
by INDIAN INSTITUTE OF TECHNOLOGY on 08/16/13. For personal use only.

The material properties of FG plates are same as being used by Shahrjerdi *et al.*,[24] and restated as follows:

Metal (Al): $\mathrm{E}_m = 68.9\,\mathrm{Gpa}$, $\upsilon = 0.33$, $\rho_m = 2\,700\,\mathrm{kg/m^3}$.

Ceramic (ZrO_2): $\mathrm{E}_c = 211\,\mathrm{Gpa}$, $\upsilon = 0.33$, $\rho_c = 4\,500\,\mathrm{kg/m^3}$.

The influence of constituents volume fraction on the natural frequencies of FG plate is studied by varying the value of material gradient index, k. As can be seen from the presented results, the natural frequencies decrease with increasing value of material gradient index, k for the same mode. For the same value of k, natural frequency increases for the higher modes. Actually, this kind of non-dimensionalization defies the physical characteristics of the frequency parameter, although mathematically it is all right. With the increase of thickness ratio (a/h) of the plate, the plates become thin, hence becoming more flexible, the fundamental natural frequency must decrease because of the decreasing stiffness of plate.

5. Concluding Remarks

In this article, a 2D plate theory for the free vibration analysis of moderately thick isotropic, orthotropic and FG elastic, rectangular plates is derived using HOSNT12. Free vibration analysis of plates with simply supported (diaphragm) edge conditions is carried out. The material properties of FG plates are assumed to vary in the thickness direction according to power law distribution. The effects of the side-to-thickness ratio, the material gradient index of constituent volume fraction on the natural frequencies are also discussed. Navier solution technique employing double Fourier series is used to get the results with desired level of accuracy. The numerical solutions are compared with the available exact 3D solutions under similar edge conditions. FG plate is modeled using power law and the obtained numerical solutions have high accuracy compared to the available 3D elasticity solutions. These high accurate numerical solutions can be used as benchmark to assess any other analytical/computational model for FG plates. The results show that the natural frequencies decrease with increasing the material gradient index as well as side-to-thickness ratios. FOST and HOST have almost the same accuracy for thin FG plates, but HOSNT12 has improved accuracy for thicker plates, therefore it is better to use this theory for thick plates. Although the presented formulation for FGM using HOSNT12 involves large computations compared to FOST and CPT, but the obtained numerical results are very accurate when compared to the 3D elasticity solutions. The benefit of this approach is that a 2D theory is able to predict solutions as good as 3D elasticity solutions.

Acknowledgments

The authors would like to thank Dr Xu Sipeng (College of Engineering, Ocean University of China, Qingdao, China) for his thorough comments involving editorial, typographical and most importantly technical, which has helped in improving the quality of the revised manuscript.

Appendix A.

Elements of plate rigidity matrices using HOSNT12

$$[\mathbf{A}]_{11\times 11} = \begin{bmatrix} I_{11,0} & I_{12,0} & I_{11,2} & I_{12,2} & I_{13,0} & 3I_{13,2} & I_{11,1} & I_{12,1} & I_{11,3} & I_{12,3} & 2I_{13,1} \\ I_{12,0} & I_{22,0} & I_{12,2} & I_{22,2} & I_{23,0} & 3I_{23,2} & I_{12,1} & I_{22,1} & I_{12,3} & I_{22,3} & 2I_{23,1} \\ I_{11,2} & I_{12,2} & I_{11,4} & I_{12,4} & I_{13,2} & 3I_{13,4} & I_{11,3} & I_{12,3} & I_{11,5} & I_{12,5} & 2I_{13,3} \\ I_{12,2} & I_{22,2} & I_{12,4} & I_{22,4} & I_{23,2} & 3I_{23,4} & I_{12,3} & I_{22,3} & I_{12,5} & I_{22,5} & 2I_{23,3} \\ I_{13,0} & I_{23,0} & I_{13,2} & I_{23,2} & I_{33,0} & 3I_{33,2} & I_{13,1} & I_{23,1} & I_{13,3} & I_{23,3} & 2I_{33,1} \\ I_{13,2} & I_{23,2} & I_{13,4} & I_{23,4} & I_{33,2} & 3I_{33,4} & I_{13,3} & I_{23,3} & I_{13,5} & I_{23,5} & 2I_{33,3} \\ I_{11,1} & I_{12,1} & I_{11,3} & I_{12,3} & I_{13,1} & 3I_{13,3} & I_{11,2} & I_{12,2} & I_{11,4} & I_{12,4} & 2I_{13,2} \\ I_{12,1} & I_{22,1} & I_{12,3} & I_{22,3} & I_{23,1} & 3I_{23,3} & I_{12,2} & I_{22,2} & I_{12,4} & I_{22,4} & 2I_{23,2} \\ I_{11,3} & I_{12,3} & I_{11,5} & I_{12,5} & I_{13,3} & 3I_{13,5} & I_{11,4} & I_{12,4} & I_{11,6} & I_{12,6} & 2I_{13,4} \\ I_{12,3} & I_{22,3} & I_{12,5} & I_{22,5} & I_{23,3} & 3I_{23,5} & I_{12,4} & I_{22,4} & I_{12,6} & I_{22,6} & 2I_{23,4} \\ I_{13,1} & I_{23,1} & I_{13,3} & I_{23,3} & I_{33,1} & 3I_{33,3} & I_{13,2} & I_{23,2} & I_{13,4} & I_{23,4} & 2I_{33,2} \end{bmatrix}, \tag{A.1}$$

$$[\mathbf{A}']_{11\times 8} = \begin{bmatrix} I_{14,0} & I_{14,0} & I_{14,2} & I_{14,2} & I_{14,1} & I_{14,1} & I_{14,3} & I_{14,3} \\ I_{24,0} & I_{24,0} & I_{24,2} & I_{24,2} & I_{24,1} & I_{24,1} & I_{24,3} & I_{24,3} \\ I_{14,2} & I_{14,2} & I_{14,4} & I_{14,4} & I_{14,3} & I_{14,3} & I_{14,5} & I_{14,5} \\ I_{24,2} & I_{24,2} & I_{24,4} & I_{24,4} & I_{24,3} & I_{24,3} & I_{24,5} & I_{24,5} \\ I_{34,0} & I_{34,0} & I_{34,2} & I_{34,2} & I_{34,1} & I_{34,1} & I_{34,3} & I_{34,3} \\ I_{34,2} & I_{34,2} & I_{34,4} & I_{34,4} & I_{34,3} & I_{34,3} & I_{34,5} & I_{34,5} \\ I_{14,1} & I_{14,1} & I_{14,3} & I_{14,3} & I_{14,2} & I_{14,2} & I_{14,4} & I_{14,4} \\ I_{24,1} & I_{24,1} & I_{24,3} & I_{24,3} & I_{24,2} & I_{24,2} & I_{24,4} & I_{24,4} \\ I_{14,3} & I_{14,3} & I_{14,5} & I_{14,5} & I_{14,4} & I_{14,4} & I_{14,6} & I_{14,6} \\ I_{24,3} & I_{24,3} & I_{24,5} & I_{24,5} & I_{24,4} & I_{24,4} & I_{24,6} & I_{24,6} \\ I_{34,1} & I_{34,1} & I_{34,3} & I_{34,3} & I_{34,2} & I_{34,2} & I_{34,4} & I_{34,4} \end{bmatrix}, \tag{A.2}$$

$$[\mathbf{B}']_{4\times 11} = \begin{bmatrix} I_{14,0} & I_{24,0} & I_{14,2} & I_{24,2} & I_{34,0} & 3I_{34,2} & I_{14,1} & I_{24,1} & I_{14,3} & I_{24,3} & 2I_{34,1} \\ I_{14,2} & I_{24,2} & I_{14,4} & I_{24,4} & I_{34,2} & 3I_{34,4} & I_{14,3} & I_{24,3} & I_{14,5} & I_{24,5} & 2I_{34,3} \\ I_{14,1} & I_{24,1} & I_{14,3} & I_{24,3} & I_{34,1} & 3I_{34,3} & I_{14,2} & I_{24,2} & I_{14,4} & I_{24,4} & 2I_{34,2} \\ I_{14,3} & I_{24,3} & I_{14,5} & I_{24,5} & I_{34,3} & 3I_{34,5} & I_{14,4} & I_{24,4} & I_{14,6} & I_{24,6} & 2I_{34,4} \end{bmatrix}, \tag{A.3}$$

$$[\mathbf{B}]_{4\times 8} = \begin{bmatrix} I_{44,0} & I_{44,0} & I_{44,2} & I_{44,2} & I_{44,1} & I_{44,1} & I_{44,3} & I_{44,3} \\ I_{44,2} & I_{44,2} & I_{44,4} & I_{44,4} & I_{44,3} & I_{44,3} & I_{44,5} & I_{44,5} \\ I_{44,1} & I_{44,1} & I_{44,3} & I_{44,3} & I_{44,2} & I_{44,2} & I_{44,4} & I_{44,4} \\ I_{44,3} & I_{44,3} & I_{44,5} & I_{44,5} & I_{44,4} & I_{44,4} & I_{44,6} & I_{44,6} \end{bmatrix}, \tag{A.4}$$

$$[\mathbf{D}]_{4\times 7} = \begin{bmatrix} I_{66,0} & I_{66,0} & 3I_{66,2} & I_{66,2} & 2I_{66,1} & I_{66,1} & I_{66,3} \\ I_{66,2} & I_{66,2} & 3I_{66,4} & I_{66,4} & 2I_{66,3} & I_{66,3} & I_{66,5} \\ I_{66,1} & I_{66,1} & 3I_{66,3} & I_{66,3} & 2I_{66,2} & I_{66,2} & I_{66,4} \\ I_{66,3} & I_{66,3} & 3I_{66,5} & I_{66,5} & 2I_{66,4} & I_{66,4} & I_{66,6} \end{bmatrix}, \tag{A.5}$$

Int. J. Str. Stab. Dyn. 2013.13. Downloaded from www.worldscientific.com
by INDIAN INSTITUTE OF TECHNOLOGY on 08/16/13. For personal use only.

Int. J. Str. Stab. Dyn. 2013.13. Downloaded from www.worldscientific.com
by INDIAN INSTITUTE OF TECHNOLOGY on 08/16/13. For personal use only.

$$[\mathbf{D}']_{4\times 7} = \begin{bmatrix} I_{56,0} & I_{56,0} & 3I_{56,2} & I_{56,2} & 2I_{56,1} & I_{56,1} & I_{56,3} \\ I_{56,2} & I_{56,2} & 3I_{56,4} & I_{56,4} & 2I_{56,3} & I_{56,3} & I_{56,5} \\ I_{56,1} & I_{56,1} & 3I_{56,3} & I_{56,3} & 2I_{56,2} & I_{56,2} & I_{56,4} \\ I_{56,3} & I_{56,3} & 3I_{56,5} & I_{56,5} & 2I_{56,4} & I_{56,4} & I_{56,6} \end{bmatrix}, \tag{A.6}$$

$$[\mathbf{E}']_{4\times 7} = \begin{bmatrix} I_{56,0} & I_{56,0} & 3I_{56,2} & I_{56,2} & 2I_{56,1} & I_{56,1} & I_{56,3} \\ I_{56,2} & I_{56,2} & 3I_{56,4} & I_{56,4} & 2I_{56,3} & I_{56,3} & I_{56,5} \\ I_{56,1} & I_{56,1} & 3I_{56,3} & I_{56,3} & 2I_{56,2} & I_{56,2} & I_{56,4} \\ I_{56,3} & I_{56,3} & 3I_{56,5} & I_{56,5} & 2I_{56,4} & I_{56,4} & I_{56,6} \end{bmatrix}, \tag{A.7}$$

$$[\mathbf{E}]_{4\times 7} = \begin{bmatrix} I_{55,0} & I_{55,0} & 3I_{55,2} & I_{55,2} & 2I_{55,1} & I_{55,1} & I_{55,3} \\ I_{55,2} & I_{55,2} & 3I_{55,4} & I_{55,4} & 2I_{55,3} & I_{55,3} & I_{55,5} \\ I_{55,1} & I_{55,1} & 3I_{55,3} & I_{55,3} & 2I_{55,2} & I_{55,2} & I_{55,4} \\ I_{55,3} & I_{55,3} & 3I_{55,5} & I_{55,5} & 2I_{55,4} & I_{55,4} & I_{55,6} \end{bmatrix}, \tag{A.8}$$

where

$$I_{ij,k} = \int_{-h/2}^{+h/2} Q_{ij} z^k dz. \tag{A.9}$$

As structural reference axes (x, y, z) of the FG plate coincide with the principal material axes (1, 2, 3) of the FG plate, thus:

$$\begin{gathered} Q_{11} = C_{11}, \quad Q_{12} = C_{12}, \quad Q_{13} = C_{13}, \quad Q_{22} = C_{22}, \quad Q_{23} = C_{23}, \quad Q_{33} = C_{33}, \\ Q_{44} = C_{44}, \quad Q_{55} = C_{55}, \quad Q_{66} = C_{66}, \quad Q_{14} = Q_{24} = Q_{34} = Q_{56} = 0. \end{gathered} \tag{A.10}$$

Appendix B.

Elements of coefficient matrix "X" using HOSNT12

$$\begin{aligned}
X_{1,1} &= A_{1,1}\alpha_m^2 + B_{1,1}\beta_n^2, & X_{2,2} &= A_{2,2}\beta_n^2 + B_{2,2}\alpha_m^2, \\
X_{1,2} &= A_{1,2}\alpha_m\beta_n + B_{1,2}\alpha_m\beta_n, & X_{2,3} &= 0, \\
X_{1,3} &= 0, & X_{2,4} &= A_{2,7}\alpha_m\beta_n + B_{1,5}\alpha_m\beta_n, \\
X_{1,4} &= A_{1,7}\alpha_m^2 + B_{1,5}\beta_n^2, & X_{2,5} &= A_{2,8}\beta_n^2 + B_{1,6}\alpha_m^2, \\
X_{1,5} &= A_{1,8}\alpha_m\beta_n + B_{1,6}\alpha_m\beta_n, & X_{2,6} &= -A_{2,5}\beta_n, \\
X_{1,6} &= -A_{1,5}\alpha_m, & X_{2,7} &= A_{2,3}\alpha_m\beta_n + B_{1,3}\alpha_m\beta_n, \\
X_{1,7} &= A_{1,3}\alpha_m^2 + B_{1,3}\beta_n^2, & X_{2,8} &= A_{2,4}\beta_n^2 + B_{1,4}\alpha_m^2, \\
X_{1,8} &= A_{1,4}\alpha_m\beta_n + B_{1,4}\alpha_m\beta_n, & X_{2,9} &= -A_{2,11}\beta_n, \\
X_{1,9} &= -A_{1,11}\alpha_m, & X_{2,10} &= A_{2,9}\alpha_m\beta_n + B_{1,7}\alpha_m\beta_n, \\
X_{1,10} &= A_{1,9}\alpha_m^2 + B_{1,7}\beta_n^2, & X_{2,11} &= A_{2,10}\beta_n^2 + B_{1,8}\alpha_m^2, \\
X_{1,11} &= A_{1,10}\alpha_m\beta_n + B_{1,8}\alpha_m\beta_n, & X_{2,12} &= -A_{2,6}\beta_n, \\
X_{1,12} &= -A_{1,6}\alpha_m,
\end{aligned}$$

$$
\begin{aligned}
&X_{3,3} = D_{1,2}\alpha_m^2 + E_{1,2}\beta_n^2, && X_{4,4} = A_{7,7}\alpha_m^2 + B_{3,5}\beta_n^2 + D_{1,1},\\
&X_{3,4} = D_{1,1}\alpha_m, && X_{4,5} = A_{7,8}\alpha_m\beta_n + B_{3,6}\alpha_m\beta_n,\\
&X_{3,5} = E_{1,1}\beta_n, && X_{4,6} = -A_{7,5}\alpha_m + D_{1,6}\alpha_m,\\
&X_{3,6} = D_{1,6}\alpha_m^2 + E_{1,6}\beta_n^2, && X_{4,7} = A_{7,3}\alpha_m^2 + B_{3,3}\beta_n^2 + D_{1,5},\\
&X_{3,7} = D_{1,5}\alpha_m, && X_{4,8} = A_{7,4}\alpha_m\beta_n + B_{3,4}\alpha_m\beta_n,\\
&X_{3,8} = E_{1,5}\beta_n, && X_{4,9} = -A_{7,11}\alpha_m + D_{1,4}\alpha_m,\\
&X_{3,9} = D_{1,4}\alpha_m^2 + E_{1,4}\beta_n^2, && X_{4,10} = A_{7,9}\alpha_m^2 + B_{3,7}\beta_n^2 + D_{1,3},\\
&X_{3,10} = D_{1,3}\alpha_m, && X_{4,11} = A_{7,10}\alpha_m\beta_n + B_{3,8}\alpha_m\beta_n,\\
&X_{3,11} = E_{1,3}\beta_n, && X_{4,12} = -A_{7,6}\alpha_m + D_{1,7}\alpha_m,\\
&X_{3,12} = D_{1,7}\alpha_m^2 + E_{1,7}\beta_n^2, && \\
&X_{5,5} = A_{8,8}\beta_n^2 + B_{3,6}\alpha_m^2 + E_{1,1}, && X_{6,6} = D_{3,6}\alpha_m^2 + B_{3,6}\beta_n^2 + A_{5,5},\\
&X_{5,6} = -A_{8,5}\beta_n + E_{1,6}\beta_n, && X_{6,7} = D_{3,5}\alpha_m - A_{5,3}\alpha_m,\\
&X_{5,7} = A_{8,3}\alpha_m\beta_n + B_{3,3}\alpha_m\beta_n, && X_{6,8} = E_{3,5}\beta_n - A_{5,4}\beta_n,\\
&X_{5,8} = A_{8,4}\beta_n^2 + B_{3,4}\alpha_m^2 + E_{1,5}, && X_{6,9} = D_{3,4}\alpha_m^2 + E_{3,4}\beta_n^2 + A_{5,11},\\
&X_{5,9} = -A_{8,11}\alpha_m\beta_n + E_{1,4}\alpha_m\beta_n, && X_{6,10} = D_{3,3}\alpha_m - A_{5,9}\alpha_m,\\
&X_{5,10} = A_{8,9}\alpha_m\beta_n + B_{3,7}\alpha_m\beta_n, && X_{6,11} = E_{3,3}\beta_n - A_{5,10}\beta_n,\\
&X_{5,11} = A_{8,10}\beta_n^2 + B_{3,8}\alpha_m^2 + E_{1,3}, && X_{6,12} = D_{3,7}\alpha_m^2 + E_{3,7}\beta_n^2 + A_{5,6},\\
&X_{5,12} = -A_{8,6}\beta_n + E_{1,7}\beta_n, && \\
&X_{7,7} = A_{3,3}\alpha_m^2 + B_{2,3}\beta_n^2 + 2D_{3,5}, && X_{8,8} = A_{4,4}\beta_n^2 + B_{2,4}\alpha_m^2 + 2E_{3,5},\\
&X_{7,8} = A_{3,4}\alpha_m\beta_n + B_{2,4}\alpha_m\beta_n, && X_{8,9} = -A_{4,11}\alpha_m\beta_n + 2E_{3,4}\alpha_m\beta_n,\\
&X_{7,9} = -A_{3,11}\alpha_m + 2D_{3,4}\alpha_m, && X_{8,10} = A_{4,9}\alpha_m\beta_n + B_{2,7}\alpha_m\beta_n,\\
&X_{7,10} = A_{3,9}\alpha_m^2 + B_{2,7}\beta_n^2 + 2D_{3,3}, && X_{8,11} = A_{4,10}\beta_n^2 + B_{2,8}\alpha_m^2 + 2E_{1,3},\\
&X_{7,11} = A_{3,10}\alpha_m\beta_n + B_{2,8}\alpha_m\beta_n, && X_{8,12} = -A_{4,6}\beta_n + 2E_{3,7}\beta_n,\\
&X_{7,12} = -A_{3,6}\alpha_m + 2D_{3,7}\alpha_m, && \\
&X_{9,9} = D_{2,4}\alpha_m^2 + E_{2,4}\beta_n^2 + 2A_{11,11}, && X_{10,10} = A_{9,9}\alpha_m^2 + B_{4,7}\beta_n^2 + 3D_{2,3},\\
&X_{9,10} = D_{2,3}\alpha_m - 2A_{11,9}\alpha_m, && X_{10,11} = A_{9,10}\alpha_m\beta_n + B_{4,8}\alpha_m\beta_n,\\
&X_{9,11} = E_{2,3}\beta_n - 2A_{11,10}\beta_n, && X_{10,12} = -A_{9,6}\alpha_m + 3D_{2,7}\alpha_m,\\
&X_{9,12} = D_{2,7}\alpha_m^2 + E_{2,7}\beta_n^2 + 2A_{11,6}, && \\
&X_{11,11} = A_{10,10}\beta_n^2 + B_{4,8}\alpha_m^2 + 3E_{2,3}, && X_{12,12} = D_{4,7}\alpha_m^2 + E_{4,7}\beta_n^2 + 3A_{6,6},\\
&X_{11,12} = -A_{10,6}\beta_n + 3E_{2,7}\beta_n, &&
\end{aligned}
\tag{B.1}
$$

where $X_{i,j} = X_{j,i}$ (for all i, j).

Appendix C.

Elements of mass matrix "M" using HOSNT12

$$
\begin{aligned}
&M_{1,1} = \Gamma_1, M_{1,4} = \Gamma_2, M_{1,7} = \Gamma_3, M_{1,10} = \Gamma_4,\\
&\qquad M_{1,2} = M_{1,3} = M_{1,5} = M_{1,6} = M_{1,8} = M_{1,9} = M_{1,11} = M_{1,12} = 0,
\end{aligned}
$$

Int. J. Str. Stab. Dyn. 2013.13. Downloaded from www.worldscientific.com by INDIAN INSTITUTE OF TECHNOLOGY on 08/16/13. For personal use only.

Int. J. Str. Stab. Dyn. 2013.13. Downloaded from www.worldscientific.com
by INDIAN INSTITUTE OF TECHNOLOGY on 08/16/13. For personal use only.

$$
\begin{aligned}
&M_{2,2} = \Gamma_1, M_{2,5} = \Gamma_2, M_{2,8} = \Gamma_3, M_{2,11} = \Gamma_4,\\
&\qquad M_{2,3} = M_{2,4} = M_{2,6} = M_{2,7} = M_{2,9} = M_{2,10} = M_{2,12} = 0,\\
&M_{3,3} = \Gamma_1, M_{3,6} = \Gamma_2, M_{3,9} = \Gamma_3, M_{3,12} = \Gamma_4,\\
&\qquad M_{3,4} = M_{3,5} = M_{3,7} = M_{3,8} = M_{3,10} = M_{3,11} = 0,\\
&M_{4,4} = \Gamma_3, M_{4,7} = \Gamma_4, M_{4,10} = \Gamma_5,\\
&\qquad M_{4,5} = M_{4,6} = M_{4,8} = M_{4,9} = M_{4,11} = M_{4,12} = 0,\\
&M_{5,5} = \Gamma_3, M_{5,8} = \Gamma_4, M_{5,11} = \Gamma_5, M_{5,6} = M_{5,7} = M_{5,9} = M_{5,10} = M_{5,12} = 0,\\
&M_{6,6} = \Gamma_3, M_{6,9} = \Gamma_4, M_{6,12} = \Gamma_5, M_{6,7} = M_{6,8} = M_{6,10} = M_{6,11} = 0,\\
&M_{7,7} = \Gamma_5, M_{7,10} = \Gamma_6, M_{7,8} = M_{7,9} = M_{7,11} = M_{7,12} = 0,\\
&M_{8,8} = \Gamma_5, M_{8,11} = \Gamma_6, M_{8,9} = M_{8,10} = M_{8,12} = 0,\\
&M_{9,9} = \Gamma_5, M_{9,12} = \Gamma_6, M_{9,10} = M_{9,11} = 0,\\
&M_{10,10} = \Gamma_7, M_{10,11} = M_{10,12} = 0,\\
&M_{11,11} = \Gamma_7, M_{11,12} = 0,\\
&M_{12,12} = \Gamma_7,
\end{aligned}
\tag{C.1}
$$

where, $M_{i,j} = M_{j,i}$ (for $i, j = 1 - 12$).

References

1. M. Koizumi, The concept of FGM, *Ceram. Trans. Funct. Grad. Mater.* **34** (1993) 3−10.
2. N. J. Pagano, Exact solutions for composite laminates in cylindrical bending, *J. Compos. Mater.* **3** (1969) 398−411.
3. N. J. Pagano, Exact solutions for rectangular bidirectional composite and sandwich plates, *J. Compos. Mater.* **4** (1970) 20−34.
4. S. Srinivas and A. K. Rao, Bending, vibration and buckling of simply supported thick orthotropic rectangular plates and laminates, *Int. J. Solids Struct.* **6**(11) (1970) 1463−1481.
5. S. Srinivas, C. V. Joga Rao and A. K. Rao, An exact analysis for vibration of simply supported homogeneous and laminated thick rectangular plates, *J. Sound Vib.* **12**(2) (1970) 187−199.
6. B. N. Pandya and T. Kant, Higher order shear deformable theories for flexural of sandwich plates: Finite element evaluations, *Int. J. Solids Struct.* **24**(12) (1988) 1267−1286.
7. T. Kant and B. S. Manjunatha, On accurate estimation of transverse stress in multilayer laminates, *Comput. Struct.* **50**(3) (1994) 351−365.
8. J. N. Reddy, *Mechanics of Laminated Composite Plates and Shells: Theory and Analysis* (CRC, New York, 1997).
9. S. Suresh and A. Mortensen, *Fundamentals of Functionally Graded Materials* (IOM Communications, London, 1998).
10. Y. Tanigawa, Some basic thermoelastic problems for nonhomogeneous structural materials, *Appl. Mech. Rev.* **48**(6) (1995) 287−300.
11. G. N. Praveen and J. N. Reddy, Nonlinear transient thermoelastic analysis of functionlly graded ceramic-metal plates, *Int. J. Solids Struct.* **35** (1998) 4457−4471.
12. J. N. Reddy, Analysis of functionally graded plates, *Int. J. Numer. Meth. Eng.* **47** (2000) 663−684.
13. R. Javaheri and M. R. Eslami, Buckling of functionally graded plates under in-plane compressive loading, *ZAMM J.* **82** (2002) 277−283.
14. R. Javaheri and M. R. Eslami, Thermal buckling of functionally graded plates, *AIAA J.* **40**(1) (2002) 162−169.

15. Z. Q. Cheng and R. C. Batra, Deflection relationships between the homogeneous Kirchhoff plate theory and different functionally graded plate theories, *Arch. Mech.* **52** (2000a) 143−158.
16. Z. Q. Cheng and R. C. Batra, Three-dimensional thermoelastic deformations of a functionally graded elliptic plate, *Compos. Part B.* **31**(1) (2000b) 97−106.
17. Z. Q. Cheng and R. C. Batra, Exact correspondence between eigenvalues of membranes and functionally graded simply supported polygonal plates, *J. Sound Vib.* **229** (2000c) 879−895.
18. S. S. Vel and R. C. Batra, Three-dimensional exact solution for the vibration of functionally graded rectangular plate, *J. Sound Vib.* **272** (2004) 703−730.
19. E. Carrera, S. Brischetto and A. Robaldo, Variable kinematic model for the analysis of functionally graded material plates, *AIAA J.* **46** (2008) 194−203.
20. L. Della Croce and P. Venini, Finite elements for functionally graded Reissner−Mindlin plates, *Comput. Meth. Appl. Mech. Eng.* **193** (2004) 705−725.
21. S. A. M. GhannadPour and M. M. Alinia, Large deflection behavior of functionally graded plates under pressure loads, *Compos. Struct.* **75** (2006) 67−71.
22. T. K. Nguyen, K. Sab and G. Bonnet, First-order shear deformation plate models for functionally graded materials, *Compos. Struct.* **83** (2008) 25−36.
23. H. Matsunaga, Free vibration and stability of functionally graded plates according to a 2-D higher-order deformation theory, *Compos. Struct.* **82** (2008) 499−512.
24. A. Shahrjerdi, F. Mustapha, M. Bayat, S. M. Sapuan, R. Zahari and M. M. Shahzamanian, Natural frequency of FG rectangular plate by shear deformation theory, *IOP Conf. Series: Materials Science and Engineering*, **17** (2011) DOI:10.1088/1757-899X/17/1/012008: 1−6.
25. J. S. Kumar, B. S. Reddy, C. E. Reddy and K. V. K. Reddy, Higher order theory for free vibration analysis of functionally graded material plates, *ARPN J. Eng. Appl. Sci.* **6** (2011) 105−111.
26. A. Benachour, H. D. Tahar, H. A. Atmane, A. Tounsi and M. S. Ahmed, A four variable refined plate theory for free vibrations of functionally graded plates with arbitrary gradient, *Compos. Part B: Eng.* **42** (2011) 1386−1394.
27. S. Xiang, Y. X. Jin, Z. Y. Bi, S. X. Jiang, M. S. Yang, A n-order shear deformation theory for free vibration of functionally graded and composite sandwich plates, *Compos. Struct.* **93** (2011) 2826−2832.
28. A. M. A. Neves, A. J. M. Ferreira, E. Carrera, C. M. C. Roque, M. Cinefra, R. M. N. Jorge and C. M. M. Soares, A quasi-3D sinusoidal shear deformation theory for the static and free vibration analysis of functionally graded plates, *Compos. Part B: Eng.* **43** (2012) 711−725.
29. A. M. A. Neves, A. J. M. Ferreira, E. Carrera, M. Cinefra, C. M. C. Roque, R. M. N. Jorge and C. M. M. Soares, A quasi-3D hyperbolic shear deformation theory for the static and free vibration analysis of functionally graded plates, *Compos. Struct.* (2012) DOI: 10.1016/j.compstruct.2011.12.005.
30. T. G. Rogers, P. Watson and A. J. M. Spencer, Exact three-dimensional elasticity solutions for bending of moderately thick inhomogeneous and laminated strips under normal pressure, *Int. J. Solids Struct.* **32** (1995) 1659−1673.
31. A. M. Main and A. J. M. Spencer, Exact solutions for functionally graded and laminated elastic materials, *J. Mech. Phys. Solids* **46**(12) (1998) 2283−2295.
32. J. N. Reddy and Z. Q. Cheng, Three-dimensional thermo mechanical deformations of functionally graded rectangular plates, *Eur. J. Mech. Solids* **20**(5) (2001) 841−855.
33. R. C. Batra and S. S. Vel, Exact solution for thermoelastic deformations of functionally graded thick rectangular plates, *AIAA J.* **40**(7) (2001) 1421−1433.
34. H. Tsukamoto, Analytical method of inelastic thermal stresses in a functionally graded material plate by a combination of a micro- and macromechanical approaches, *Compos. Part B*, **34**(6) (2003) 561−568.

Int. J. Str. Stab. Dyn. 2013.13. Downloaded from www.worldscientific.com
by INDIAN INSTITUTE OF TECHNOLOGY on 08/16/13. For personal use only.

35. M. Kashtalyan, Three-dimensional elasticity solution for bending of functionally graded rectangular plates, *Eur. J. Mech. Solids* **23** (2004) 853–864.
36. V. P. Plevako, On the theory of elasticity of inhomogeneous media, *J. Appl. Math. Mech.* **35**(5) (1971) 806–813.
37. E. Reissner, The effects of transverse shear deformation on bending of elastic plates, *ASME J. Appl. Mech.* **12** (1945) A69–A77.
38. R. D. Mindlin, Influence of rotary inertia and shear in flexural motions of isotropic elastic plates, *ASME J. Appl. Mech.* **18** (1951) 1031–1036.
39. T. Kant, Numerical analysis of thick plates, *Comput. Meth. Appl. Mech. Eng.* **31** (1982) 1–18.
40. T. Kant and B. S. Manjunatha, An unsymmetric FRC laminate C^0 finite element model with 12 degrees of freedom per node, *Eng. Comput.* **5**(3) (1988) 300–308.
41. S. Timoshenko and J. Goodier, *Theory of Elasticity* (McGraw Hill, New York, 1951).
42. J. N. Reddy and A. A. Khdeir, Buckling and vibration of laminate composite plates using various plate theories, *AIAA J.* **27** (1989) 1808–1817.
43. J. N. Reddy, A refined nonlinear theory of plates with transverse shear deformation, *Int. J. Solids Struct.* **20**(9/10) (1984) 881–896.
44. J. N. Reddy and N. D. Phan, Stability and vibration of isotropic, orthotropic and laminated plates according to a higher-order shear deformation theory, *J. Sound Vib.* **98**(2) (1985) 157–170.
45. T. Kant and K. Swaminathan, Free vibration of isotropic, orthotropic and multilayer plates based on higher order refined theories, *J. Sound Vib.* **241**(2) (2001) 319–327.
46. R. P. Shimpi and H. G. Patel, A two variable refined plate theory for orthotropic plate analysis, *Int. J. Solids Struct.* **43** (2006) 6783–6799.
47. H. Reisman and Y. C. Lee, Forced motions of rectangular plates, *Develop. Theor. Appl. Mech.* **4** (1969) 3.

Int. J. Str. Stab. Dyn. 2013.13. Downloaded from www.worldscientific.com
by INDIAN INSTITUTE OF TECHNOLOGY on 08/16/13. For personal use only.